# ~~Forest fire risk assessment in Sweden using climate model data: bias correction and future changes~~Multi-variable bias correction: application of forest fire risk in present and future climate in Sweden

**W. Yang[1], M. Gardelin[1], J. Olsson[1], and T. Bosshard[1]**

[1]{Swedish Meteorological and Hydrological Institute, Norrköping, Sweden}

Correspondence to: W. Yang (wei.yang@smhi.se)

## Abstract

As the risk for a forest fire is largely influenced by weather, evaluating its tendency under a changing climate becomes important for management and decision making. Currently, biases in climate models make it difficult to realistically estimate the future climate and consequent impact on fire risk. A distribution-based scaling (DBS) approach was developed as a post-processing tool that intends to correct systematic biases in climate modelling outputs. In this study, we used two projections, one driven by historical reanalysis (ERA40) and one from a global climate model (ECHAM5) for future projection, both having been dynamically downscaled by a regional climate model (RCA3). The effects of the post-processing tool on relative humidity and wind speed were studied in addition to the primary variables precipitation and temperature. Finally, the Canadian Fire Weather Index system was used to evaluate the influence of changing meteorological conditions on the moisture content in fuel layers and the fire-spread risk. The forest fire risk results using DBS are proven to better reflect risk using observations than that using raw climate outputs. For future periods, southern Sweden is likely to have a higher fire risk than today, whereas northern Sweden will have a lower risk of forest fire.

## 1 Introduction

A forest fire is an uncontrolled fire event. It can exert a destructive influence on ecosystems, affecting climate and weather (Flannigan, 2009). ~~In summer 2014, the largest forest fire in Sweden since at least the mid-1900s occurred in the county of Västmanland, causing damages~~

~~valued at around 1 billion SEK (Skydd & Säkerhet, 2014).~~ On the other hand, it also has beneficial effects on wilderness areas where some species depend on prescribed fire for growth and reproduction (Brockway and Lewis, 1997) and on fire hazard reduction (Fernandes and Botelho, 2003).

Forest fire activity is strongly affected by two factors: weather conditions and availability of fuels. The weather conditions directly and indirectly affect fire behaviour during both ignition and burning by influencing the fuel conditions, especially through the moisture content in the uppermost dead fuel (Fosberg and Deeming, 1971). Over the past century, global warming caused by an anthropogenic increase in greenhouse gases has shown its impact on present climate (IPCC, 2007). This is likely to have even more of an impact if these gases continue to increase with human activities. The changing climate will thus likely accelerate the water cycle on a global scale, subsequently intensify the uneven distribution of precipitation, and cause more extreme weather conditions locally (IPCC, 2013). Studying the changes in fuel conditions caused by changing climate is hence important for decision making, both for public authorities and in forest management.

In an international context, the forest fire risk in Sweden is limited. Owing to efficient fire suppression, during years with average or low fire hazard the total annually burnt area of forest is commonly not exceeding 5000 ha since 1950s. However, during the high-hazard years the burnt area can be substantial, for instance, the fires in Gotland (1992, 1 000 ha), Tyresta (1999, 450 ha), Bodträskfors (2006, 1900 ha), Hassela (2008, 1300 ha) and the most recent one in Sala (2014, ~14000 ha) that caused damages valued at around 1 billion SEK (http://sv.wikipedia.org/wiki/Skogsbranden_i_V%C3%A4stmanland_2014 and Skydd & Säkerhet, 2014). Today, most of the ignitions are human caused, followed by lightning ignition (Granström, 1993). Extreme weather condition such as the conditions prior and during the Sala fire (i.e., extremely low relative humidity, strong wind speed and extreme high temperature) is also one of causes that make fuels conductive to ignition and spread (Fendell and Wolff, 2011; Ryan, 2002). Dendrochronological fire studies have indicated a large temporal and spatial variability in fire activity in Sweden during the last 500 years (Niklasson and Granström, 2000; Drobyshev et al., 2014). A recent study by Drobyshev et al. (2014) reveals that a geographical division between one northern and one southern region with different characteristic fire activity could be found around 60° N.

In climate change studies, global climate models (GCMs) and regional climate models (RCMs) are widely used tools to simulate climate at different scales. RCMs in general outperform GCMs in many aspects due to 1) a better representation of geographical features such as orography thanks to finer spatial resolution (typically at 25–50 km) and 2) a better description of physical processes by means of, e.g., sub-grid scale parameterisation and more detailed land surface schemes (Giorgi and Marinucci, 1996; Samuelsson et al., 2010). However, the mismatch between RCM-simulated and observed climatological conditions still cannot be neglected. A study conducted by the Swedish Commission on Climate and Vulnerability (SOU, 2007) demonstrated the limitations of using raw data from a climate model for forest fire danger estimation, as historically simulated fire danger levels were consistently lower compared to risk levels estimated using meteorological observations. This discrepancy is very likely caused by biases in driving variables from climate model outputs.

One conventional approach to tackle climate model bias is the Delta Change method (DC) by which an observed data time series is perturbed with a projected climate change (Flannigan et al., 1991; Stocks et al., 1998; Hay et al., 2000). Typically, the changes in long-term climatology on a monthly or seasonal basis are superimposed on the observation records over the entire frequency distribution, i.e., for both extreme and normal events. This approach is easy to implement and keeps exactly the same change in climatological mean in meteorological variables as that in climate projection, but with two limitations. The first limitation is that only average change in monthly variables is incorporated. The variance in future climate comes either from observed data or from perturbed data, but it does not directly come from climate projection. The second limitation is that changes in regional climate (i.e., one grid cell) are assumed to be the same for all locations in the same region, which is very unlikely to be true. Another widely used approach in forest fire risk studies is built on the statistical relationship of weather conditions at the point scale (i.e., single station) and at its corresponding climate model grid cell (Mearns et al., 1995; Logan et al., 2004). The approach has been applied in a number of case studies (Bergeron and Flannigan, 1995; Wotton et al., 2003). By this approach, various correction processes were designed for different variables: 1) precipitation frequency and humidity magnitude are corrected using the statistical relationship identified under present climate; 2) noon temperature is simply estimated as modelled maximum daily temperature minus 2.0 ºC; 3) wind speed comes directly from model output and remains uncorrected. This approach makes model output more realistic for use in fire risk studies; however, it merely treats a small part of the bias in variables in a simple way. That is,

the frequency of rainy days is corrected but not precipitation magnitude; humidity variables are corrected in terms of long-term mean but without consideration of variance; no treatment is carried out for bias in modelled maximum daily temperature and wind speed.

Recently, the quantile-mapping approach has been developed to correct bias in climate model outputs. The approach mainly focuses on correcting the biases in precipitation (and/or temperature) from RCMs to better reflect observations via mapping either parametric or non-parametric cumulative distribution functions (CDFs) to observed and projected climate variables (Piani et al., 2010; Themeßl et al., 2010; Yang et al., 2010). A few studies have focused on correcting RCM bias in other hydrologically relevant meteorological variables, e.g., relative humidity, wind speed and solar radiation (Wilcke et al., 2013).

This study presents work regarding the forest fire risk in Sweden under changing climate. The forest fire model, observations and climate data are introduced in section 2. The systematic bias originated from RCMs is removed by one of the quantile-mapping approaches, the distribution-based scaling (DBS), which is extended to support bias correction of wind speed and relative humidity (See section 3). Following the experimental set-up in section 4, the newly developed approach was calibrated and validated, and then further applied to the impact study. Ultimately, an impact study was carried out via two RCM simulations, one reanalysis-driven historical run for method development and validation under present climate and one GCM-driven future projection for estimating the climate change impact. Their corresponding results are discussed in section 5. At the end of the paper, some conclusions and remarks on future development are given in section 6.

## 2 Fire risk model and data

### 2.1 Fire Weather Index System (FWI)

The Fire Weather Index system, FWI, is a major component of the Canadian Forest Fire Weather Danger Rating System (Stocks et al., 1989). It was originally designed for a standardised forest type in Canada and has lately been used for fire danger estimation by many other countries (Viegas et al., 1999; Carvalho et al., 2008).

The details of the application of the FWI can be found in Van Wagner (1987) and Dowdy et al., 2010. Here, only the key features of each component are summarized. The FWI system

tracks daily moisture content variations in three stratified fuel layers in forests ~~(Fig. 1)~~, coded as primary indices: the Fine Fuel Moisture Code (FFMC), the Duff Moisture Code (DMC) and the Drought Code (DC). For every index, two phases are considered: rainfall phase and drying phase. They are determined by a threshold value given as an empirical value in the FWI literature for the purpose of each index~~: 0.5 mm rainfall for the FFMC, 1.5 mm rainfall for the DMC and 2.8 mm for the DC~~. Any rainfall below the threshold value is to be ignored in individual layers. As the three layers differ in fuel type and in their connections to the weather conditions in the proximity, they play different roles in potential fire behaviour. What they have in common are the influencing factors. They are present as moisture content in the fuel, drying rate and weather states of being dry or wet (i.e., rainy or non-rainy day). ~~The details of the application of the FWI can be found in Van Wagner (1987).~~

### 2.1.1 ~~Fine fuel Moisture Code~~ Primary indices: FFMC, DMC and DC

The uppermost surface layer, described by the FFMC, responds rapidly to the short-term changes in weather conditions that are described by precipitation, P [mm], temperature, T [º C], relative humidity, $H$ [%] and wind speed, $W$ [km $h^{-1}$]. It is the most important layer in the FWI and other fire risk models when assessing fire risk.

~~$$FFMC = (147.2 \times 101 - 59.5mc)/(mc + 147.2) \quad (1)$$~~

~~where $mc$ [%] is moisture content in the fuel. The drying rate, $k$ [$\log_{10}$ % $day^{-1}$], is computed as a function of temperature, relative humidity and wind speed by following Eqs. (2) and (3):~~

~~$$k_d = 0.424\left[1 - (H/100)^{1.7}\right] + 0.0694W^{0.5}\left[1 - (H/100)^{8}\right] \quad (2)$$~~

~~and~~

~~$$k_w = 0.424\left[1 - \left(\frac{100 - H}{100}\right)^{1.7}\right] + 0.0694W^{0.5}\left[1 - \left(\frac{100 - H}{100}\right)^{8}\right] \quad (3)$$~~

~~$$k = 0.581e^{0.0365T}k_d \,(or\ k_w) \quad (4)$$~~

~~where $k_d$ indicates the log drying rate at the normal temperature of 21.1 ºC and $k_w$, is named as the log wetting rate, which accounts for the process of atmospheric wetting at high humidity. Considering the temperature effect, the final log drying (or wetting) rate is computed as shown in Eq. (4). Finally, $mc$ in the fuel is calculated by Eqs. (5) or (6), depending on the~~

~~difference between the magnitude of the moisture content in fuel and the equilibrium moisture content, $E$ [%], determined by relative humidity and temperature in the environment:~~

~~$mc = E_d + (mc_0 - E_d)10^{-k_d}$ (5)~~

~~$mc = E_w + (E_w - mc_0)10^{-k_w}$ (6)~~

~~where $E_d$ and $E_w$ are the equilibrium moisture contents for drying and for wetting and $mc_0$ stands for previous day's moisture content.~~

### ~~2.1.2 Duff Moisture Code~~

The middle layer is a loosely compacted organic layer on the forest floor. The DMC was designed to reflect its average moisture content. It gives an indication of the slow-drying forest fuel consumed in burning. This layer is influenced by all input variables except wind speed. Again, the moisture content, $mc$ [%], is an indicator to reflect the moisture condition in the fuel.~~:~~

~~$DMC = 244.72 - 43.43\ln(mc - 20)$ (7)~~

Differently from the computation in the FFMC layer, the drying rate, $k$ [$\log_{10}$ % day$^{-1}$], in the DMC layer is calculated as proportional not only to temperature and the deficit in relative humidity but also to the day length varying with season, $L_e$ [hours].~~, as shown in Eq. (8):~~

~~$k = 1.894(T + 1.1)(100 - H)L_e 10^{-6}$ (8)~~

### ~~2.1.3 Drought Code~~

The bottom layer is a very slow-drying compact organic fuel in the deeper soil layers. Its corresponding code, DC, reflects the influence of long-term drying on the fuels (Turner, 1972). It is used to detect extremely long dry conditions in lower layers of deep duff, which may result in persistent smouldering. ~~DC is calculated as:~~

~~$DC = 100\ln(800/Q)$ (9)~~

~~where $Q$ [0.01 inch] is the moisture equivalent.~~

This layer does not have direct contact with the atmosphere. It only absorbs moisture through rainfall and dries out through the evapotranspiration process. Therefore, its final code computed from moisture equivalent is a function of the previous code value and potential evapotranspiration, $V$ [~~0.01 inch~~mm/day]:

~~$DC = DC_0 + 0.5V$ (10)~~

~~$V = 0.36(T + 2.8) + L_f$ (11)~~

~~where $L_f$ [-] is the seasonal daylength adjustment and $DC_\theta$ stands for previous day's DC value.~~

### ~~2.1.4~~2.1.2 Integral indices: Build-Up Index, Initial Spread Index and Fire Weather Index

The Build-Up Index (BUI) and the Initial Spread Index (ISI) are two intermediate sub-indices computed based on the aforementioned primary moisture indices. They were designed to describe the fire behaviours, the available fuel and the rate of fire spread for combustion. BUI is built up by the combination of the DMC and the DC. It indicates all fuel available for consumption during the burning process. ISI is computed by combining moisture content in the fine fuel and *W* using a wind function, *f (W)*, and a fine fuel moisture function, *g (FFMC)* (Van Wagner, 1987). It is used as an indicator for the potential rate of fire spreading.

~~$ISI = 0.208\, f(W)\, g(FFMC)$ (12)~~

~~$BUI = 0.8 DMC \times DC / (DMC + 0.4 DC)$ (13)~~

Ultimately, the Fire Weather Index (FWI) is an integrated function of a function of ISI, *h (ISI)*, and a function of ISI, *l (BUI)*, to represent fire intensity as energy output rate per unit length of fire front.

~~$FWI = h(ISI) \times l(BUI)$ (14)~~

### ~~2.1.5~~2.1.3 Application of the FWI system in Sweden

At SMHI, the original FWI system has been run operationally since 1998. ~~Fire danger classes (FWIX) for different FWI ranges have, however, been corrected to be suitable for Swedish conditions (Table 1) (Gardelin, 1997).~~ In Gardelin (1997), the FWI model was evaluated by comparison with forest fire statistics in the eastern parts of Kalmar and Jönköping County where 675 fires were reported from 1989 to 1994. Fire danger classes (FWIX) for different FWI ranges have, however, been corrected to be suitable for Swedish conditions (Table 1) (Gardelin, 1997). Since 1999 ~~T~~the system is used to make nationwide fire risk forecasts at 11 x 11 km resolution during the fire season from April to October. The estimated fire risks serve as the basis for general forest fire warnings to the public, rescue services and emergency

centres in Sweden. Previous studies concluded that the original FWI system generally works well for Swedish conditions (Gardelin, 1997; Granström and Schimmel, 1998). Strong relationships between index levels (FFMC, DMC and DC) and measured moisture content were found. The relationships are highly varying depending on the fuel types. Additionally, the final FWI index well represented the forest fire statistics in terms of number of fires and burnt area for the forest fire-prone regions during past and present climate in Sweden. The FWI system is therefore chosen for climate change impact studies.

## 2.2 Data

### Observations

Data from meteorological stations with observed 24-h accumulated precipitation (*P*-obs) as well as temperature (*T*-obs), wind speed (*W*-obs) and relative humidity (*H*-obs) at 12UTC were compiled, covering a reference period from 1966 to 2005. They were extracted from the Swedish network of observation stations (see Fig. ~~2~~1) with at least 30-year long measurements with less than 20% missing values in the reference period, to ensure coverage of various climate phenomena~~asignificant statistical properties~~. The following requirements were considered: 1) geographically evenly distributed to represent most of the Swedish climatic regions; 2) observations of high quality. It should be emphasised that wind speed is inherently hard to measure in a consistent way over long time periods because the instruments are repositioned, nearby buildings are put up or torn down; forests grow up or get cut, etc. Nevertheless, some findings can be summarized by analysing the observations, which will be described in section 5.1.1.

### RCM simulations

Two climate simulations, denoted as RCA3-ERA40 and RCA3-E5r3-A1B, were used in this study. They were both dynamically downscaled to 25 km resolution by the RCM, the RCA3, but driven by different large-scale forcing data as lateral boundaries. The RCA3 is the 3$^{rd}$ full release of the Rossby Centre Regional Climate model, developed at the Swedish Meteorological and Hydrological Institute (SMHI) (Samuelsson et al., 2010). For many near-surface variables, the RCA3 represents the European climate well when compared to other RCMs (Hagemann et al., 2004).

The RCA3-ERA40 simulation uses the ERA40 reanalysis data as its boundary condition and covers the period from 1961 to 2000. It is assumed to represent the reality as represented by local observations and was therefore used to verify the methodology in this paper. The RCA3-E5r3-A1B transient projection from 1961-2100 is based on the ECHAM5 GCM (Roeckner et al., 2006), forced with the IPCC emissions scenario A1B, an intermediate scenario with respect to the magnitude of future global warming (Nakicénović et al., 2000). In this experiment, the RCA3-E5r3-A1B projection was first evaluated for past climate and then used for future impact assessment. Within the ensemble of 16 climate projection studies by Kjellström et al. (2011), RCA3-E5r3-A1B represents projections in the small-to-medium range with respect to the expected future increase of both P and T.

The same variables as those collected at observation stations were extracted for the following experiment. They are grid-averaged daily precipitation (*P*-raw), 2 m temperature (*T*-raw), 2 m relative humidity (*H*-raw) and 10 m wind speed (*W*-raw). Time series from the RCA3 grid cell covering each of the stations were used.

## 3 RCM bias correction for fire risk modelling

The DBS method is a parametric quantile-mapping approach. It aims to correct systematic bias in GCM/RCM outputs while preserving the temporal variability in meteorological variables resulting from climate projections over time. In DBS, as opposed to common non-parametric quantile-mapping approaches, meteorological variables are fitted to appropriate parametric distributions that allow for generation of values outside the range of the reference period and thus simulation of previously unobserved conditions in future climate periods.

The general form of the DBS approach is:

$$x_{Sim}^{Corr} = F_{Obs}^{-1}\left[F_{Sim}(x_{Sim}^{Org}, \gamma_{Sim,}\varphi_{Sim}), \gamma_{Obs}, \varphi_{Obs}\right] \quad (1)\text{~~(15)~~}$$

where $\gamma$ and $\varphi$ are distribution parameters estimated from the climate model (subscript Sim) and from the observations (subscript Obs) by the Maximum Likelihood Estimator (MLE), the method of moments, iterative or other approximate methods; $x_{Sim}^{Org}$ is the original output of variable x simulated by a climate model and $x_{Sim}^{Corr}$ is the result after correction. $F_{Sim}$ and $F_{Obs}^{-1}$ stand for the cumulative distribution function (CDF) and its inverse of a suitable parametric distribution for each variable of interest.

The distribution parameters of precipitation are estimated for every season, whereas the distribution parameters of other variables are estimated using a 31-day moving window for every Julian day, and fourier series are used to describe the distribution parameters over the year in a smooth way:

$$\gamma(t^*) = \frac{a_0}{2} + \sum_{k=1}^{K}\left[a_k \cos(kwt^*) + b_k \sin(kwt^*)\right] \quad (2)\ \text{~~(16)~~}$$

$$\varphi(t^*) = \frac{c_0}{2} + \sum_{k=1}^{K}\left[c_k \cos(kwt^*) + d_k \sin(kwt^*)\right] \quad (3)\ \text{~~(17)~~}$$

where $a_0$, $a_k$, $b_k$, $c_0$, $c_k$ and $d_k$ are the Fourier coefficients, $t^*$ is the day of the year; $w$ equals $2\pi/n$, where n is the time units per cycle (in our case 365 days) and $k$ stands for the $n^{th}$ harmonic. Theoretically, (t*/2 + 1) harmonics are able to represent a complete cycle perfectly, with the drawback of a potential overfitting of the data. Five harmonics have been found to be sufficient in Yang et al. (2010).

### 3.1 DBS for P and T: an overview

A detailed description of the DBS for P and T correction can be found in a previous study by Yang et al. (2010). In the following, only a summary is given.

To tackle the common RCM bias in terms of the overestimated frequency of rainy days with small rainfall amount (i.e., wet frequency bias, “drizzle effect”) a cut-off value is identified as a threshold to correct the frequency of rainy days (P > 0.1 mm) in climate projections. Any drizzle, generated by the RCM model, with intensity smaller than the threshold is removed, and the day with the drizzle is treated as a dry day. Dry frequency bias, i.e., the tendency of RCMs to underestimate wet-day frequency, is rather uncommon in Europe but may occur, e.g., during summer in south-eastern Europe and in the Alps (Hagemann et al., 2004; Jacob et al., 2007). In the current DBS method, such wet-day deficit is handled by adding a small rainfall amount at the end of wet spells, starting with the longest ones, until the correct frequency is obtained. In-depth analysis and research work are progressing.

After the precipitation frequency bias has been corrected, the remaining modelled precipitation is then transformed to match the distribution of observed precipitation. The full time series is divided into two partitions separated by the $95^{th}$ percentile identified from sorted observation records and model simulation. This approach intends to capture the main

properties of normal low-to-medium-intensity precipitation as well as the high-intensity extremes. A double-gamma distribution, instead of a conventional gamma distribution, is accordingly implemented. Two sets of parameters – $\alpha$, $\beta$ (normal precipitation) and $\alpha_{95}$, $\beta_{95}$ (extremes) – are estimated by the Maximum Likelihood Estimator (MLE) from observations and from the RCM output in the reference period. The fitted scaling parameters are then applied to correct the RCM outputs for the entire projection period by Eq. (1~~5~~). For impact studies in Europe, four seasons are normally used. They are winter (Dec-Feb), spring (Mar-May), summer (Jun-Aug) and autumn (Sep-Nov).

Daily temperature values are described using a Gaussian distribution. For every Julian day, the distribution parameters, $\mu_T$ and $\sigma_T$, are estimated from observations and RCM data. Considering the dependency between P and T, the statistics of temperature are calculated separately for wet days (i.e., rainy days) and dry days (i.e., non-rainy days).

### 3.2 DBS for H and W: method development

The approach for correcting *H* and *W* is similar to that for daily *P* and *T*. The factors used to scale *H* and *W* were defined conditioned on the location of the station and the season of interest. For wind speed scaling, the precipitation state (i.e. wet or dry) is considered as an influencing factor.

Relative humidity is different than other variables in that its value is restricted to the interval of [0, 1]. To cope with this property, the commonly used Beta distribution (Yao, 1974) is chosen, the density distribution of which is:

$$f(x) = \left[\frac{\Gamma(p+q)}{\Gamma(p)\Gamma(q)}\right] x^{p-1}(1-x)^{q-1} \qquad \text{~~(4)(18)~~}$$

where $p$ and $q$ are the two parameters of the distribution and $\Gamma$ is the gamma function. By different combinations of $p$ and $q$, a wide range of distribution shapes maybe represented. The distribution parameters can be fitted by the method of moments using the equations below:

$$\mu = \frac{p}{p+q} \qquad \text{~~(5)(19)~~}$$

$$\sigma^2 = \frac{p\,q}{(p+q)^2(p+q+1)} \qquad \text{~~(6)(20)~~}$$

where $\mu$ and $\sigma$ are the statistical mean and standard deviation of the data to be fitted.

The Beta density function is not analytically integrable; however, its cumulative probability, F, can be obtained through numerical methods by using the incomplete Beta function (Abramowitz and Stegun, 1984; Press et al., 1986).

Wind speed is an atmospheric variable characterised by properties that are similar to precipitation, i.e., positive skewness and non-negative property. It is commonly described by the Weibull distribution (Pavia and O'Brien, 1986; Seguro and Lambert, 2000). Its density distribution is given as:

$$f(x) = \left(\frac{\kappa}{\lambda}\right)\left(\frac{x}{\lambda}\right)\exp\left[-\left(\frac{x}{\lambda}\right)^{\kappa-1}\right] \qquad \kappa, \lambda, x \succ 0 \qquad (7)\text{~~(21)~~}$$

where the two parameters $\kappa$ and $\lambda$ are shape and scale parameters, respectively. The shape parameter, $\kappa$, describes numerous shapes with different magnitudes of positive skewness, while the scale parameter, $\lambda$, controls the stretch of the distribution.

The Weibull distribution has several special forms when setting the shape parameter $\kappa$ to different values. For instance, the Weibull distribution is identical to the gamma distribution when $\kappa$ equals 1, and it is very similar to the Gaussian distribution when $\kappa$ equals 3.6. It can also be transformed to be an Extreme Value Distribution (EVD) with location parameter $\mu$ = *log* ($\kappa$) and scale parameter $\sigma = \lambda^{-1}$. Because of its particular properties, it can also be used to solve other distributions after transformation. The distribution parameters of the Weibull distribution are conventionally estimated using MLE. As its density function is analytically integrable, as expressed in Eq. (~~22~~8), it is straight-forward to calculate the probability and solve the inverse function:

$$F(x) = 1 - \exp\left[-\left(\frac{x}{\lambda}\right)^{\kappa}\right] \qquad \kappa, \lambda, x \succ 0 \qquad (8)\text{~~(22)~~}$$

## 4 Experimental set-up and evaluation

RCM-simulated *P*-raw, *T*-raw, *H*-raw and *W*-raw at 12 UTC were bias-corrected using observations from meteorological stations (see Section 3). Along with original outputs from RCMs and observed variables, the corrected variables were used to drive the FWI system for assessing forest fire danger. The internal variables (FFMC, DMC, DC) as well as the

integrated indices BUI, ISI, the final index (FWI), and the fire danger level (FWIX) were all used for evaluating the influence of the DBS approach.

To validate the approach, 1966-1985 (20 years) was used as the calibration period for both simulations; 1986-2000 (15 years) was used as the validation period for the RCA3-ERA40 simulation (as the reanalysis data i.e., ERA40 ends by 2000), and 1986-2005 (20 years) was used for the RCA3-R3E5-A1B simulation. Basic statistics such as the climatological mean (Avg) and the standard deviation ($SD^1$) were calculated in both the calibration and validation periods. For P, the seasonal mean (Acc) is used to present its long-term mean. Because of discrete-continuous property of precipitation and wind speed, an additional statistic, the frequencies of rainy and windy days are computed to study how the model captures their properties. In the following, they are denoted as Freq-P (i.e. occurrence of days with rainfall amount larger than 0.1 mm) and Freq-Ws (i.e. occurrence of days with wind speed above 0 m $s^{-1}$). Moreover, a standard distance ($SD^2$) was included to investigate the spatial variations of every variable. It is computed as the standard deviation of the mean values of all stations. A larger value indicates a higher variability in space, and vice versa.

Apart from that, how well climate models can capture the observed probability distribution of individual variables was also studied using a PDF Skill Score (SS) (Perkins et al., 2007). The SS is a quantitative assessment of goodness-of-fit in terms of probability distribution to evaluate the consistency between two data sets. The results reflect the agreement, with a perfect agreement resulting in an SS of 1.0 and a poor agreement in an SS close to 0. In this work, the SS is calculated from observation, raw and corrected RCM outputs. Its formula is expressed as in Eq. (~~23a~~9a) and (~~23~~9b), where m is the number of bins used to calculate the PDF for a given variable per station, $Z_{raw}$ (and $Z_{corrected}$) is the probability in a given bin from model simulation before and after bias correction, respectively, and $Z_{Obs}$ is the probability in a given bin from the observed data.

$$SS_{raw} = \sum_{1}^{m} \min\left(Z_{raw}, Z_{Obs}\right) \quad \text{(9a)(~~23a~~)}$$

$$SS_{corrected} = \sum_{1}^{m} \min\left(Z_{corrected}, Z_{Obs}\right) \quad \text{(9b)(~~23b~~)}$$

All these statistics were calculated from the climate projections' output before and after bias correction, and observations. For *P*, *H* and *W*, their relative differences in Avg were used for bias evaluation, whilst for *T*, the differences in Avg were used. In terms of the two SD ($SD^1$

and $SD^2$), the ratio of their values calculated from model outputs and from the observations was used to identify the differences in describing the variances.

For future climate change (CC) assessment, the scaling parameters obtained from the reference periods (i.e., 1966–1995) were applied to individual variables for the future periods in climate projections. Subsequently, the corrected variables were used to run the FWI system. The transient future projections were divided into three 30-year time periods – 2011–2040, 2041–2070, 2071–2100 – for analysing the climate change signals and influence of the DBS method on meteorological variables and further on the forest fire danger in near, intermediate and distant futures. The results for the period, 2071-2100, are to be presented in this paper.

This paper focuses on the results for the period from March to November, a typical fire period for Europe. Thus, the three seasons MAM (Mar-May), JJA (Jun-Aug) and SON (Sep–Nov) are studied in the following. One station – Edsbyn – is used to illustrate the results from the DBS correction, and another station – Växjö – is used to present the climate change impacts.

# 5 Results and discussion

## 5.1 Evaluation for present climate

### 5.1.1 Meteorological variables

Sweden is characterised as a mixture of temperate and continental climate with four distinct seasons. The seasonal temperature varies on average from – 4 °C in winter (not shown here) to 18.3 °C in summer (see Table 2). Due to its large coverage in latitude, the temperature in Sweden varies greatly from north to south, with 12 ºC difference in winter temperature and 6 ºC difference in summer temperature (not shown here).

Precipitation in Sweden occurs throughout the whole year. In general, it often rains less in spring and winter, whereas it rains heavily in summer and autumn with stronger variability. The rainfall frequency in spring is in the same range as that in summer, but approximately 21 % less compared to that in autumn; however, the accumulative precipitation amount in spring is much lower compared to the other two seasons (i.e. 42.8 % compared to summer and 50.6 % compared to autumn), which implies drier conditions in spring (see Table 2 and Fig. ~~3~~2).

In terms of relative humidity, the distribution varies from season to season. On average, the relative humidity in Sweden appears to be relatively low in spring and summer (i.e., in the range of 55 – 65 %) and reaches its minimum value in summer. From autumn onward, its value continuously increases until its annual maximum in winter (see Table 2, Fig. ~~3~~ 2 and ~~4~~3).

Annual mean wind speed in Sweden varies between 2 and 5 m $s^{-1}$, with an average of 4 m $s^{-1}$. In southern Sweden it is generally high because this region is more exposed to westerly and south-westerly wind. Wind speed closer to the coast features stronger variability than that in the inner region. Wind speed in the inner regions of central Sweden such as Edsbyn is characterised as a general weak annual cycle with the weakest wind in winter (see Fig. ~~3~~2).

With respect to its spatial distribution (see $SD^2$ in Table 2) precipitation is a localised variable, while the rest of the variables are largely influenced by large-scale effects.

As reanalysis data (i.e., ERA40) is generally assumed to be the closest dataset to the real climate, the deviations from observations in the RCA3-ERA40 run are considered to mainly reflect RCA3 model bias. The main findings from a comparison between observed and RCA3-ERA40 simulated climate statistics include the following (see Tables 2 and 3):

- The seasonal precipitation amount is generally overestimated for all three seasons, whereas variability is in general slightly lower than that of the observations (see $Std^1$ in Table 2). The climate model estimates the frequency of wet days with the lowest accuracy for summer, in which almost 100% bias was found in comparison to the observations; the overestimation in autumn was 66.7 % and in spring it was 80.8 %. The average SS had a value of 0.60. Again, the summer precipitation is the least accurately simulated, with an SS value of approximately 0.56 (See Table 3). Concerning spatial variability, modelled precipitation tends to be more unevenly distributed than observations in spring and summer, which is in contrast to the situation in autumn.

- A cold bias appears during all fire seasons. The largest bias (-2.3 °C) was found in summer, whereas the lowest bias (-0.9 °C) appeared in autumn. This is also reflected by the SS being 0.80 for spring, 0.85 for autumn and 0.71 for summer (See Table 3). Similar to precipitation, the spatial variability at point stations is underestimated by

the climate model in autumn (-7.7 %), whereas it is overestimated by ~30 % in spring and summer.

- The variability of relative humidity is in general well reproduced, being within -2.5 ~ +6.1 % of the observed variance. However, the magnitude in summer is overestimated by 18.8 %. The largest deviation of relative humidity is found in summer, followed by autumn and spring. The climate model generates more days with higher Rh-raw than in the observations. The high SS for spring (i.e., 0.81) indicates a good match between simulation and observation, but the skill scores for summer (0.72) and autumn (0.74) are relatively lower (See Table 3). Again, an overestimated spatial variability (i.e., 148.4 % in spring and 36.4 % in summer) is found in the modelled data for the fire season except for autumn (-14.3 %).
- Wind speed and its variance are evidently underestimated during all seasons of interest. Its distribution is positively skewed but with a larger proportion of low wind speeds and a smaller proportion of high wind speeds in the simulated data (Fig. ~~4~~3). In the RCM run, Ws-raw of more than 6 m $s^{-1}$ seldom occurs, which differs from those in the observations in which speeds up to 15 m $s^{-1}$ occur. The SS is on average 0.70 (See Table 3). In contrast to the other variables, for modelled wind speed the $SD^2$ is significantly lower (~ -75%) than that in the observations. Such a damped spatial variability is noted in all fire seasons, as shown in Table 2.
- Summer is always the season with the largest bias.

One source of bias is the mismatch of spatial scale between station data (point scale) and RCA3 grid cells (25×25 km). Compared to a GCM (~ 200 km) the spatial resolution of the RCMs is clearly more suited for approximating local conditions, but still the difference in statistical characteristics between point scale and averages over thousands of $km^2$ is huge for highly spatially varying variables, notably precipitation and wind. It should be emphasized that bias is also caused by measurement errors and uncertainties, e.g. precipitation undercatch, incorrect temperature observations in cold conditions and changing surroundings affecting wind gauges.

Apart from that, the biases are also likely caused by limitations in the climate models' process descriptions. Biases in precipitation may be linked to an overestimation of cloud fraction in mountainous areas (Willén, 2008), incorrectly solved convective triggering and lack of details in geographical information, which lead to unrealistic precipitation simulation. The cold bias

(~-2°C) in summer and in autumn over northern Europe may be partly because of an overestimation of cloud water by the RCA3, which leads to too much shortwave radiation being reflected and subsequently an underestimation of the incoming shortwave radiation at the surface (Willén, 2008). Additionally, the bias in relative humidity in summer may be due to overestimated cloud water that subsequently leads to an underestimation of maximum summer temperatures over Northern Europe (Samuelsson et al., 2010). In terms of wind speed, a general bias is noted when comparing model output to long-term climatological means. This can be attributed to the parameterization utilized in unresolved orography, and uncaptured small scale features, for instance, the influence of hills, lakes, valleys, etc. Furthermore, the incorrect seasonal wind speed variation generated by the climate model implies that the RCA3 model well captures large-scale forcing but no other influencing processes such as seasonal variations and atmospheric stability over land and water that largely influence the wind speed (Achberger et al., 2006). For inland stations, such as Edsbyn, the seasonal variation in stability over the land is smaller than that over the sea, which reduces the seasonal wind speed variation compared to stations close to the sea (Achberger et al. 2006). However, it seems that Edsbyn was modelled as a coastal location where winter wind speed is enhanced because of less stably stratified atmosphere over water and the stronger pressure gradient in winter.

Bias in GCM-forced RCM runs reflects the integral influence of GCM and RCM. In comparison of the two RCA3 simulations, the reanalysis-forced run (i.e., RCA3-ERA40) is found to outperform the GCM-forced run (i.e., RCA3-E5R3A1B), however, the difference is overall small and their annual cycles are very similar (see Fig. ~~3~~2). As shown by the statistics in Table 2 and frequency distribution in Fig. ~~4~~3, the RCA3-E5R3A1B generally performs similarly or worse in terms of the statistical mean and variability. The largest differences appear for precipitation simulation for which RCA3-E5R3A1B generated up to 105% higher wet-day percentage and 118 % more accumulated precipitation than present in the observations in summer. In terms of precipitation frequency distribution RCA3-ERA40 tends to generate a slightly higher number of days with small rainfall amount and fewer days with extreme amounts. Temperature is another variable with visible difference between the two simulations. Again, the largest differences appear in summer in which RCA3-E5r3-A1B is inclined to be slightly colder and with less variability than RCA3-ERA40. The distributions of relative humidity and wind speed generated from two simulations are in general almost identical.

Though the two climate projections are driven by different forcing, many of their characteristics are highly consistent, implying that the majority of the biases are likely to originate from the RCM. The alternative conclusion would be that the ERA40 is as bad as the GCM in simulating the statistics of these four variables.

As the climate projection forced by GCM is the basis for assessing future impact, we will mainly focus on evaluating the results from RCA3-E5r3-A1B in the following.

### 5.1.2 Effect of the DBS approach

Fig. ~~5~~ 4 and ~~6~~ 5 illustrate how the DBS method improves the FWI input variables. In the calibration period (not shown here) the bias-correction effectively removed the majority of biases in all of the variables, which is expected as the bias-correction parameters have been calibrated on the same set of data. In the following we will focus the analysis on the validation period to illustrate the effect of DBS.

The correction was first applied to the two primary variables, P and T. The cut-off values obtained from the parameter estimation process for precipitation scaling (see Section 3.1) range from 0.6 to 3.2 mm over all stations during the fire seasons. The largest cut-off value always appears in summer, followed by autumn and then spring. At station Edsbyn, the cut-off value varies from 0.85 mm/day (spring) to 1.56 mm/day (summer). After removing the bias, the corrected P shows a better match with observed data over all three seasons, though partial biases in volume still remain, as shown by Fig. ~~5~~4. The improvement in temperature is noticeable in terms of both the full distribution and the annual cycle. The major improvement occurs for summer and spring where the cold bias appears in modelled data. The corrected T is statistically equivalent to that from the observations in terms of climatological mean and standard deviation of temperature conditioned on dry and wet days. As with temperature, the corrected relative humidity shows a better annual distribution. The overestimation of relative humidity is largely reduced, but some bias still remains at the tail of the distribution. Wind speed gets substantially improved in terms of both magnitude and annual distribution. The overestimated number of days with small wind speeds is reduced, and the probability of higher wind speed is largely improved, but the DBS-corrected data tends to overestimate the wind speeds over 6 m $s^{-1}$. Taking a closer look at the PDF of meteorological variables from different data sources by comparison of Fig. ~~4~~ 3 and Fig. ~~6~~5, we find that the effect of the DBS largely depends on the performance of raw climate projections. Whether the climate

model is capable of reflecting the changes between the calibration and validation period is very significant. In observation time series, the local climate at the station Edsbyn is found to be warmer (except for summer) and wetter (except for autumn) in the validation period than that in the calibration period. The largest rise in temperature appears in winter (i.e., 2.2 ºC), followed by a large rise in spring (i.e., 0.9 ºC) and a moderate rise in autumn (i.e., 0.4 ºC). In summer, the temperature is found to drop by 0.7 ºC. For precipitation the seasonal precipitation is found to be wetter in spring (i.e., 4.3 %) and summer (i.e., 13.3 %), but drier in winter by 14.0 % and in autumn by 11.7 % (not shown here). In the climate model's output (i.e., the R3E5A1B) for the same period a similar trend for temperature is found but with smaller magnitude; however a different trend for precipitation is found. The climate model simulates generally wetter conditions in the validation period over the whole year with a rise of more than 10 % per season except for autumn (i.e., 6.6 %). The increment in spring and summer may even reach 15.0 % and 13.6 %. That is, the climate model does not correctly capture the trend in variables and also largely overestimates their changing rate. As a result, unstable statistics in raw climate projections make it difficult to obtain a correction as good as in the calibration period, which subsequently leads to an imperfect match in fire risk index, e.g., the DC in Fig. ~~7~~6.

Apart from computed statistics, the distribution corrections are also reflected by the SS. The SS in Table 4 show general improvement in all variables, i.e., the SS are on average ~ 0.93 for precipitation, ~ 0.90 for temperature, ~ 0.83 for relative humidity and 0.83 for wind speed, though the seasons differ. The largest improvements appear in the summer season in which the major biases tend to occur in the raw climate projections. Similar improvement has been found when the correction was applied to the RCA3-ERA40 run (not shown here).

### 5.1.3 Forest fire risk indices

The major forest fire risk indices – FFMC, DMC, DC, BUI, ISI and FWI – are plotted as long-term average annual cycles over the calibration (1966–1985) and the validation (1986–2005) periods in Fig. ~~7~~ 6 and ~~8~~7.

The calculated fire risk indices using raw RCA3 outputs are at first studied in comparison to those obtained using station data. The deviation (see blue and black lines in Fig. ~~7~~ 6 and ~~8~~7) is intuitively understandable. Too many drizzle days in the raw RCA3 data are very likely to cause oversaturation in the soil that may not dry out between rainfall events as in the

reference simulation driven by station data. Furthermore, along with lower temperature, the water content in the deepest fuel layer might be increased, affecting long-term drying conditions of the soil. Higher relative humidity as well as lower wind speed leads to a decrease of the drying rate. As a whole, moisture content in the uppermost layer is overestimated and the corresponding fire risk described by the FFMC index is underestimated (Fig. ~~7~~6). Similar effects also work on the slow-drying fuel layer (DMC) and the deepest fuel layer (DC). Because of the unrealistic values of the DMC and DC indices, the modelled BUI and ISI are also, as expected, far from the observed (Fig. ~~8~~7). Ultimately, the final FWI is substantially underestimated. Correction of input variables is thus of uttermost importance when climate projections are utilised for forest fire risk assessment.

The DC is an integrating index reflecting the combined effect of precipitation and temperature; it was therefore used to study the correcting impact induced by the DBS on these two variables. As the rainfall cut-off values for all stations are seldom above 2.8 mm (i.e., the threshold values given in the FWI literature, described in section 2.1), the major impact on the DC values is considered to be from the correction of *P* and *T*. During the drying phase, the moisture depletion is governed by evapotranspiration, which is proportional to noon temperature and also influenced by the seasonal day-length. During the rainfall phase, any rainfall more than the threshold value is first reduced to an effective rainfall by a linear function and then simply added to the existing moisture equivalent. After bias was removed, the corrected noon temperature was in general increased, which led to stronger evapotranspiration. Additionally, the reduction of precipitation amounts (see Fig. ~~5~~ 4 and ~~6~~5) resulted in less moisture equivalent. Ultimately, the fire risk in the slowly-acting fuel, described by the DC value, was found to be considerably enlarged in comparison to that which was computed using raw climate output (see Fig. ~~7~~6) as well as closer to that computed using observations.

The DMC represents the moisture content of real slow-drying forest fuel. It is a function of precipitation, temperature and relative humidity. For the RCA3-R3E5A1B the cut-off values for the summer season (i.e., JJA) are often more than 1.5 mm (i.e., the threshold values given in the FWI literature, described in section 2.1), but seldom in other seasons. Therefore, for summer, not only precipitation amount but also precipitation frequency will affect the DMC value. After applying the DBS, *H* became less overestimated and the cold bias in noon temperature was removed (see Fig. ~~5~~ 4 and ~~6~~5), which led to the larger drying rate. For the

rainfall phase the DBS not only removed the small rainfall events but also reduced the portion of medium-size rainfalls via correcting the precipitation distribution (see Fig. ~~5~~ 4 and ~~6~~5). As a result, the overestimated moisture level and consequently also the integral value of the DMC were corrected (see red line in Fig. ~~7~~6). In comparison to the DMC value computed by corrected *P* and *T* (i.e., denoted as corrected PT and marked as green line in Fig. ~~7~~6), correcting *H* and *W* (red line) leads to additional improvement. Especially in summer and autumn seasons, the maximum improvement reaches as much as 50 %. It is likely because of the removal of drizzle in the precipitation frequency correction which reduced the moisture content in the fuel.

The FFMC reflects the integrated effect of all meteorological input variables. In the drying phase, its drying rate varies with temperature, relative humidity and wind speed. After applying the DBS the drying rate was increased upon correcting the cold bias in T, the overestimated *H* and the underestimated *W*, as shown in Fig. ~~5~~ 4 and ~~6~~5. Moreover, the computed equilibrium moisture content by drying and by wetting, $E_d$ and $E_w$, became smaller (not shown here). In the rainfall phase, only the current moisture content and rainfall amount matter. As the cut-off values estimated at all stations were all above 0.5 mm (i.e. the threshold values given in the FWI literature, described in section 2.1), any correction of precipitation frequency influenced the final FFMC value. By applying the DBS, many periods of drizzle were removed and the overestimated precipitation amount was corrected. As a result, 1) the wet spells were shortened and the moisture content in the fuels had time to dry out; 2) the fire risks described by the FFMC value largely increased (see red line in Fig. ~~7~~6).

In Fig. ~~8~~7, the fire behaviour indices, the ISI and the BUI, as well as the final fire risk index, the FWI, were studied. As ISI is a product of wind speed and fine fuel moisture, it is directly influenced ~~reflects directly~~ when these two are changed. As the *W* was not perfectly corrected, over- or underestimated *W* after bias correction caused larger variation in the ISI index in comparison to that computed using observations. BUI depends on the variation in the DMC and the DC values, with more weight given to DMC. Hence, the BUI shows a similar pattern to the DMC index. Ultimately, the final index, the FWI (Fig. ~~8~~7), and the fire danger classes, the FWIX (Fig. ~~9~~8), used for issuing fire risk warnings (i.e. danger class > = 5 in Table 1) were significantly improved.

The fire risk related indices generally showed improvement when all variables were corrected compared to only a partial bias-correction of precipitation and temperature. This suggests that

the bias-correction does not destroy the physical consistency between the variables in such a way that it would degrade the validation results when multiple variables are bias-corrected. Apart from that, the improvements imply that the relative humidity and wind speed do play important roles in final fire danger level and appropriate correction of these two variables adds value to fire risk assessment. Particularly, the wind speed works as a dominant factor for cases of extremely large forest fire risk (see danger class >= 5 in Fig. ~~9~~8). This finding matches the conclusion drawn from a recent study in Greece (Karali et al., 2014), in which a ~~sensitive~~ sensitivity test of the FWI indices to the meteorological variables was carried out. It was found that precipitation and wind speed play the most important roles in final indices. Specifically, for wind speed, even a moderate wind speed leads to index values over the critical risk thresholds, and a high wind speed results in an extremely high value of the FWI.

Figure 10 gives an overview of how often the high risk indices of forest fire (i.e., FWI >= 5) are likely to occur in past climate (1966-1995) at the 14 stations used in this study. Colour markers indicate the average number of days with the FWI index of 5 and 6 per fire season (the months of April to October). At most stations, the occurrence of high risk indices derived from simulations forced by observed data are less than 20 days per fire season. In the southern parts of Sweden the high risk indices of forest fire appear more frequently, whereas in northern and central Sweden the occurrence of high risk indices are lower except at the station Edsbyn (i.e., 20 days per fire season). In comparison with the risk level calculated using the observations, the risk level calculated using raw meteorological variables from the climate projection, R3E5A1B, shows obvious underestimation. No high risk level is reflected at any of 14 stations (shown in Fig. ~~10b~~11b). After correcting the biases in meteorological variables, the fire risk in the reference period is significantly increased and it shows a similar spatial distribution pattern to that calculated from observations (see Fig. ~~10a~~ 11a and c). However, underestimation in the calculated occurrence of high risk indices (i.e., an average of -6 days per fire season) still exists. None of the stations reaches the number of days identified from those calculated using the observations. The maximum number of days calculated using corrected meteorological variables is 20 days.

## 5.2 Future projection (RCA3-E5r3-A1B)

The climate projection was run until the end of 2100 with a transient mode simulation, which makes it possible to investigate the evolution of climate change in a continuous manner (Kjellström et al. 2006). The historical observations used to obtain the scaling factors cover

the period from 1966 to 1995, the longest observation period available for the study area. Topics that will be discussed in this section include whether the DBS alters the climate change signals in input variables as well as the FWI index and how fire risk will evolve in Sweden in the future.

Figure 9 ~~11 and Figure 12~~ presents the climate change signals in all input variables at two stations, Edsbyn in northern Sweden and Växjö in southern Sweden. As projected by RCA3-E5r3-A1B, the local climate in Edsbyn will become wetter, warmer, more humid and slightly windier in the future. During fire seasons, a general increase in the precipitation amount is found during the complete future period, particularly during spring in the intermediate and distant future (~40% increase). Temperature and relative humidity are also characterised by a general rise during the whole period. The air gets warmer and moister at the beginning of spring in the near future and this tendency is enhanced until 2100. The largest rise appears in spring and the smallest in summer. Compared to the present climate, it is likely to be warmer by ~~2 ºC (~~5 ºC~~)~~ in ~~2011-2040 (~~2071-2100~~)~~ and moister by ~~8 % (~~15 %~~)~~ in ~~2011-2040 (~~2071-2100~~)~~. The change in wind speed is smaller when compared to other variables. It varies mainly within the range of -6 % to 6 % in the study periods, with the largest increase in the near future. The maximum increase appears in autumn in every future period. The local changes in Växjö are projected to be similar to those in Edsbyn, but with stronger seasonal variations during the fire season. As in Edsbyn, temperature and relative humidity exhibit a consistent future increase. Their rate of increase increases with time until 2100 (i.e., ~~1.5 °C (~~4 ºC~~)~~ warmer ~~until 2011–2040 (2071–2100)~~ and ~~5% (~~15 %~~)~~ moister until ~~2011–2040 (~~2071–2100~~)~~). The changes of the other two variables fluctuate around zero with a different sign at different period of the year. Precipitation decreases during the fire season except in spring, whereas wind speed increases in late summer with a maximum of 10 %.

In general, the corrected data ~~well~~ reproduce the climate change signal in the raw climate model output reasonably well. However, in some cases DBS was found to alter the changes projected by the climate model. It might be caused by non-linearity in RCM biases. That is, the biases caused by an imperfect model representation of atmospheric physics for the present climate are likely to be altered by the changes in relevant climatic variables in the future. For instance, the described changes in temperature bias can be related to changes in cloud cover and the corresponding response in radiative surface heating, soil moisture feedback and sea

level pressure (Maraun, 2012), which are not accounted for in the bias correction approach. As all bias correction methods, applying DBS is built upon an assumption of stationary bias.

By running the FWI system, the integral impact on the long-term mean future fire risk danger was evaluated (Fig. ~~13~~10). Because the figures aim to present the average situations for ~~every~~ 30-year period, extreme values cannot be seen. However, their relative changes in FWI compared to that for the present climate is quite consistent though different in magnitude. The differences in CC signal between the raw and DBS-corrected data, respectively, are partly because of biases in driving variables as described in section 5.1.3. Moreover, as the three primary indices of the FWI (i.e., FFMC, DMC and DC) are computed for drying and wetting phases that are determined by a threshold value for each fuel, any correction of precipitation amount may have an impact on the indices that subsequently influences the final index, FWI, and its CC signals.

Using the corrected data, ~~early spring~~autumn at the Edsbyn station is found to become more prone to forest fire, followed by spring~~autumn~~, and then summer (~~top panel in~~ Fig. ~~13~~10). It is mainly due to the increase of temperature and wind speed. For today's main fire risk season, summer, the relative change in the FWI value tends to be negative~~. In the near future, the fire risk level is likely to reduce by 20% at the end of spring and the beginning of summer. In the intermediate future, the risk in early summer becomes even lower~~ (i.e., approximately ~~-50~~ -20 %). ~~It recovers in late summer and keeps increasing up to 30 % in the last 30 years of the century.~~ The moister air, the increased precipitation and relatively stabilised wind speed balance out the effect from warmer climate. The fire risk in autumn gradually increases with regard to the last 30 years, particularly the beginning of autumn, which is most likely because of relatively drier and warmer air combined with stronger wind speeds. At the Växjö station ~~(bottom panel in Fig. 13)~~, the most fire prone season in future is likely to be summer where less precipitation, warmer temperatures and higher wind speeds are projected. ~~In the near future, the fire risk in summer rises by 5 % because of less precipitation ( -16 %) and higher wind speed (10 %), whereas the fire risk in spring drops by 10% because of increased precipitation and slightly increased relative humidity, which may probably balance out the effect of slightly increased temperature and wind speed during the same period. In the intermediate future, both precipitation and wind speed decrease, which keeps the fire risk level in summer at a consistent high level (3%) until the end of autumn. In contrast to the summer, increased precipitation and relative humidity make the fire risk level in spring even~~

~~lower (-2 %) than that in the near future.~~ In the last 30 years, the local climate gets even wetter, moister and less windy in spring, which reduces the fire risk level by 15 % compared to the present day. However, the fire risk in summer increases by ~~10~~ 20 % as the climate in the distant future becomes drier, warmer and windier.

The relative changes in the number of days with high fire risk (i.e., the FWI >=5) during the fire season are presented in Fig. ~~14~~11d. Northern Sweden is likely to be a fire resistant region in the future climate where the number of days with high fire risk is found to be lower than today. In contrast, southern Sweden is projected to become a more fire prone region where an increased number of days with high fire risk is found in almost all stations in all three periods. The stations located in central Sweden are projected to face an increased risk of forest fire in the near future, after which the risk decreases until end of the century. The changes at those stations vary from time to time, which is probably because of local climate factors at different time periods.

## 6 Conclusions

In this study, two climate projections driven by different forcing were investigated for direct use of a climate model (i.e., GCM or GCM/RCM) in forest fire risk studies. The raw climate model outputs show a clear mismatch with the observations in all influencing variables used in fire risk modelling: precipitation, temperature, wind speed and relative humidity. This is likely caused by uncertainties in observations as well as improper descriptions of physical processes and coarse resolutions in the present generation of RCMs.

Two parametric distributions were tested for correcting the biases in relative humidity (a Beta distribution) and wind speed (a Weibull distribution). In a cross-validation, the DBS method is demonstrated to substantially reduce the bias in driving meteorological variables and thus facilitates the utilisation of climate projections in forest fire risk studies. Regarding the simultaneous bias-correction of multiple variables, the result showed an improved description of fire-risk related indices when all variables were corrected compared to only a partial bias-correction of precipitation and temperature. This suggests that the bias-correction does not destroy the physical consistency between the variables to such an extent that it degrades the validation results when multiple variables are bias-corrected.

For the present climate, by using bias-corrected meteorological variables the FWI model generates realistic results that are well in line with those derived from observations. The frequency of extremely high fire risk is significantly better reproduced when compared to directly using raw climate projection data, though some underestimation remains. Further development of the DBS method is therefore required to, e.g., better represent the influencing variables by removing remaining biases, keep consistency amongst meteorological variables in terms of their temporal and spatial covariance, and capture the non-stationaries of climate model biases.

Concerning the future climate, the climate projection used here projects a climate in Sweden that is warmer, wetter and windier than today. Southern Sweden, where it is normally warmer and windier than in other parts of Sweden, is likely to become a more fire prone region in the future, whereas northern and central Sweden will face a similar or lower fire risk than today. Forest fire activity and its spread is a result of combinations of weather, fuels and topography as well as incident management decisions. Thus, fuel bed structure and fire potential are influencing factors in addition to the changing climate. This kind of studies for Sweden has been partly done previously (Granström et al., 2000 and Granström and Schimmel, 1998). With changing climate, there may be a northward displacement of the broad vegetation belts with an increasing component of broad-leaved tree species at the expense of spruce (Koca et al., 2006). Fuel beds in the north may then shift from moss to leaf litter, with unknown effects on ignition potential and fire behavior. Apart from reducing human-caused ignition, experience concerning rescue tactics suppression methods need to be collated. An ongoing project will develop a national preparedness strategy for forest fires with consideration of changing climate.

Our results do not completely agree with the work of Flannigan et al. (2013), who found significant increases in the Northern Hemisphere by applying a combination of three GCMs and three emission scenarios. For Sweden, an overall and large increase was projected. One reason for the differences may be the way the climate change signal is treated. The DBS approach focuses on preserving the variability produced by individual climate projection, which is different from the traditional delta change (DC) approach by which the average changes are transferred onto the observations. Another difference concerns the spatial and temporal resolutions of the observed reference data. Compared to the large-scale data used in

Flannigan et al., 2013, using regional/local data is beneficial in studies including localized variables such as precipitation and wind speed.

Forest fire regimes with different climatic sensitivity in northern and southern Sweden have also been revealed in earlier studies. The results in Drobyshev et al. (2014) pointed towards the presence of two well-defined zones with characteristic fire activity, geographically divided at approximately 60º N. Such division was also reflected in Dai et al. (2012) who applied the self-calibrated Palmer drought severity index to study the global aridity in present and future climate. The calculated indices indicated drier conditions in southern Sweden than in the northern part under present climate. In the future, more precipitation was projected in northern Sweden in comparison with relative dryness in the southern Sweden.

For improved interpretation of the assessment results, all uncertainties in the full production chain must be considered. Reliance on a single climate projection (combination of GCM and RCM) to represent the current and future climate is not sufficient given the amount of uncertainty involved in the climate models themselves. As forest fire is largely affected by weather conditions in close proximity and influencing forcing is very local, including different projections is required for forest fire impact assessment. A full-scale evaluation of the future forest fire risk should include an ensemble of projections covering different aspects such as parameterisation of sub-grid scale processes in GCMs and RCMs, initialisation of GCMs, spatial resolutions and emission scenarios. Also, other uncertainty sources should be assessed. One concerns the quality of observation data, which limits the application of the bias correction method to the climate projections. Another source is the choice of bias correction method, which is likely to influence the results. Finally, the choice of forest fire model adds uncertainty. For example, the connection between fuel layers is switched off in the drying process within the FWI, whereas in other models (e.g., Fosberg, 1975) a more complete drying model that couples heat and vapour transport is included. The way a model describes the processes may potentially give a different response to the projected driving meteorological variables.

## Acknowledgements

This work was mainly funded by the Swedish Civil Contingencies Agency (MSB), through project Klimatscenarier Brandrisk FWI (contract no. 2009/729/180) and Klimatpåverkan på skogsbrandrisk i Sverige. Nulägesanalys, modellutveckling och framtida scenarier (contract

no. 2011-3777). Additional funding was provided by the Swedish EPA (Naturvårdsverket), through project CLEO (contract no. 802-0115-09), the Swedish Research Council Formas, through project HYDROIMPACTS2.0 (contract no. 2009-525) and EU FP7, through project IMPACT2C (contract no. 282746). The authors would like to thank Johan Andreásson, Jörgen Sahlberg and Björn Stensen for their support in this study.

## References


Abramowitz, M., and Stegun, I.A.: Pocketbook of mathematical functions, Verlag Harri Deutsch, Frankfurt, 468 pp., 1984.

Achberger, C., Chen, D.L., and Alexandersson, H.: The surface winds of Sweden during 1999-2000, Int. J. Climatol., 26, 159-178, 2006.

Bergeron, Y. and Flannigan, M.D.: Predicting the effect of climate change on fire frequency in the southeastern Canadian boreal forest, Water, Air and Soil Pollution 82, 437-444, 1995.

Brockway, D.G and Lewis, C.E.: Long-term effects of dormant-season prescribed fire on plant community diversity, structure and productivity in a longleaf pine wiregrass ecosystem. Forest Ecology and Management, Vol. 96, Issues 1–2, 167-183, 1997.

Carvalho, A., Flannigan, M.D., Logan, K., Miranda, A.I. and Borrego, C.: Fire activity in Portugal and its relationship to weather and the Canadian Fire Weather Index System, International Journal of Wildland Fire, 17, 328-338, 2008.

Dai, A.: Increasing drought under global warming in observations and models,

Nature Climate Change, 3(1), 52-58, doi:10.1038/nclimate1633, 2013.

Dowdy, A. J., Mills, G.A., Finkele, K. and de Groot, W. J.: Australian fire weather as represented by the McArthur Forest Fire Danger Index and the Canadian Forest Fire Weather IndexRep., 84 pp, Centre for Australian Weather and Climate Research, 2009.

Drobyshev, I., Granström, A., Linderholm, H.W., Hellberg, E., Bergeron, Y. and Niklasson,

20 M.: Multi-century reconstruction of fire activity in Northern European boreal forest 21 suggests 21 differences in regional fire regimes and their sensitivity to climate, Journal of 22 Ecology, 22 Volume 102, Issue 3, 738–748, doi: 10.1111/1365-2745.12235, 2014.

Fendell, F.E. and Wolff, M.F.: Wind-Aided Fire Spread, Forest Fires, Behavior and

24 Ecological Effects, Edward A. Johnson and Kiyoko Miyanishi (eds) Chapter 6, pp171-

25 223, 2001.

Fernandes, P.M. and Botelho, H.S.: A review of prescribed burning effectiveness in fire hazard reduction, International Journal of Wildland Fire 12(2), 117 – 128, 2003.

Flannigan, M.D. and Van Wagner, C.E.: Climate change and wildfire in Canada, Canadian Journal of Forest Research, 21, 66-72, 1991.

Flannigan, M.D., Amiro, B.D., Logan, K.A., Stocks, B.J. and Wotton, B.M.: Forest Fires and Climate Change in the 21st century, Mitigation and Adaptation Strategies for Global Change 11, 847-859, 2009.

Flannigan, M., Cantin, A. S., de Groot, W. J., Wotton, M., Newbery, A. and Gowman, L. M.: Global wildland fire season severity in the 21st century, Forest Ecology and Management, 294, 54-61, doi:10.1016/j.foreco.2012.10.022, 2013.

Fosberg M.A., and Deeming J.E.: Derivation of the 1 and 10-hour timelag fuel moisture calculations for fire danger rating. U. S. Department of Agriculture, Forest Service, Research Note RM-207, Rocky Mountain Forest Experimental Station, Fort Collins, Colorado, 1971.

Fosberg, M. A.: Heat and water vapour flux in conifer forest litter and duff: A theoretical 11 model, Rep. RM-152, 23 pp., For. Serv., U.S. Dep. of Agric., Washington, D. C, 1975

Gardelin, M.: Brandriskprognoser med hjälp av en kanadensisk skogsbrandsmodell, Räddningsverket Report, Myndigheten för samhällsskydd och Beredskap (MSB), Sweden, 1997.

Giorgi, F. and Marinucci, M. R.: Improvements in the simulation of surface climatology over the European region with a nested modelling system, Geophys. Res. Lett. 23, 273–276, 1996.

Granström, A.: Spatial and Temporal variation in lightning ignitions in Sweden. J. Vegetation 18 Sci. 4, 737-744, 1993.

Granström, A., and Schimmel, J.: Utvärdering av det kanadensiska brandrisksystemet – Testbränningar och uttorkningsanalyser, Räddningsverket, Myndigheten för samhällsskydd och Beredskap (MSB), Sweden, 1998.

Granström, A., Berglund, L. and Hellberg, E.: Gräsbrand. Uttorkning och brandspridning i 23 relation till brandriskindex. Grass fuels in Northern Sweden. Moisture relations and fire 24 spread in relation to fire-weather indicies. Räddningsverket Report, Myndigheten för 25 samhällsskydd och Beredskap (MSB), Sweden, 2000.

Hagemann, S., Machenhauer, B., Jones, R., Christensen, O.B., Déqué, M., Jacob, D. and Vidale, P.L.: Evaluation of water and energy budgets in regional climate models applied over Europe, Clim. Dyn., 23, 547-567, 2004.

Hay, L.E., Wilby, R.L., and Leavesley, G.H.: A comparison of delta change and downscaled GCM scenarios for three mountainous basins in the United States, J. Am. Water Resour. As., 36, 387-398, 2000.

IPCC (2007): Climate Change: Synthesis Report. Contribution of Working Groups I, II and III to the Fourth Assessment Report of the Intergovernmental Panel on Climate Change. IPCC, Geneva, Switzerland, 104 pp., 2007.

IPCC, 2013: Climate Change 2013: The Physical Science Basis. Contribution of Working 8 Group I to the Fifth Assessment Report of the Intergovernmental Panel on Climate Change 9 [Stocker, T.F., D. Qin, G.-K. Plattner, M. Tignor, S.K. Allen, J. Boschung, A. Nauels, Y. Xia, 10 V. Bex and P.M. Midgley (eds.)]. Cambridge University Press, Cambridge, United Kingdom 11 and New York, NY, USA, 1535 pp, doi:10.1017/CBO9781107415324, 2013.

Jacob, D., Bärring, L., Christensen, O.B., Christensen, J.H., de Castro, M., Déqué, M., Giorgi, F., Hagemann, S., Hirschi, M., Jones, R., Kjellström, E., Lenderink, G., Rockel, B., Sánchez, E., Schär, C., Seneviratne, S.I., Somot, S., van Ulden, A., and van den Hurk, B.: An inter-comparison of regional climate models for Europe: model performance in present-day climate, Climatic Change, 81, 31-52, 2007.

Karali, A., Hatzaki, M., Giannakopoulos, C., Roussos, A., Xanthopoulos, G. and Tenentes, V.: Sensitivity and evaluation of current fire risk and future projections due to climate change: the case study of Greece, Nat. Hazards Earth Syst. Sci., 14, 143-153, doi:10.5194/nhess-25 14-143-2014, 2014.

Koca, D., Smith, B. and Sykes, MT.: Modelling regional climate change effects on potential 22 natural ecosystems in Sweden, Climatic Change, 78, 381-406, 2006.

Kjellström, E., Bärring, L., Gollvik, S., Hansson, U., Jones, C., Samuelsson, P., Rummukainen, M., Ullerstig, A., Willén, U. and Wyser, K.: A 140-year simulation of European climate with the new version of the Rossby Centre regional atmospheric climate model (RCA3), SMHI Rep. Meteorol. Climatol., 108, Swedish meteorological and hydrological institute (SMHI), Sweden, 2006.

Kjellström, E., Nikulin, G., Hansson, U., Strandberg, G. and Ullerstig, A.: 21st century changes in the European climate: uncertainties derived from an ensemble of regional climate model simulations, Tellus 63A, 24-40, doi: 10.1111/j.1600-0870.2010.00475.x, 2011.

Logan, K. A., Flannigan, M. D., Wotton, B. M. and Stocks, B. J.: Development of daily weather and fire danger scenarios using two general circulation models, in: Proceedings 22nd Tall Timbers Fire Ecology Conference: Fire in temperate, boreal, and montane ecosystems, edited by: Engstrom, R.T., Galley, K.E.M., and de Groot, W.J., Kananaskis Village, Alberta, Canada. Tall Timbers Research, Inc., Edmonton, Alberta, Canada (Imperial Printing Ltd.). 185-190, 2004.

Maraun, D.: Nonstationarities of regional climate model biases in European seasonal mean temperature and precipitation sums, Geophys. Res. Lett., 39, L06706, doi: 10.1029/2012GL051210, 2012.

Mearns, L.O., Giorgi, F., McDaniel, L. and Shields, C.: Analysis of daily variability of precipitation in a nested regional climate model: comparison with observations and doubled CO2 results, Global and Planetary Change, 10, 55–78, 1995.

Nakicénović, N., Alcamo, J., Davis, G., de Vries, B., Fenhann, J., Gaffin, S., Gregory, K., Gruebler, A., Jung, T.Y., Kram, T., La Rovere, E. L., Michaelis, L., Mori, S., Morita, T., Pepper, W., Pitcher, H., Price, L., Riahi, K., Roehrl, A., and Rogner, H.-H.: IPCC Special Report on Emissions Scenarios, Cambridge University Press, Cambridge, UK, New York, NY, USA, 2000.

Niklasson, M. and Granström, A.: Numbers and sizes of fires: Long term trends in a Swedish 19 boreal landscape. Ecology 81, 1496-1499, 2000.

Pavia, E.G., and O'Brien, J.J.: Weibull statistics of wind speed over the ocean, J. Clim. Appl. Meteorol., 25, 1324– 1332, 1986.

Perkins, S.E., Pitman, A.J., Holbrook, N.J., and McAneney, J.: Evaluation of the AR4 Climate Models' Simulated Daily Maximum Temperature, Minimum Temperature, and Precipitation over Australia Using Probability Density Functions, J. Climate, 20, 4356–4376, 2007.

Piani, C., Haerter, J.O., and Coppola, E.: Statistical bias correction for daily precipitation in regional climate models over Europe, Theor. Appl. Climatol., 99, 187-192, 2010.

Press, W.H., Flannery, B.P., Teukolsky, S.A., and Vetterling, W.T.: Numerical Recipes: the Art of Scientific Computing, Cambridge University Press, Cambridge, UK, 818 pp., 1986.

Roeckner, E., Brokopf, R., Esch, M., Giorgetta, M., Hagemann, S., Kornblueh, L., Manzini, E., Schlese, U. and Schulzweida, U.: Sensitivity of simulated climate to horizontal and vertical resolution in the ECHAM5 atmosphere model, J. Climate, 19, 3771–3791, 2006.

Ryan KC.: Dynamic interactions between forest structure and fire behaviour in boreal 5 ecosystems, Silva Fennica 36: 13-39, 2002.

Samuelsson, P., Jones, C.G., Willén, U., Ullerstig, A., Gollvik, S., Hansson, U., Jansson, C., Kjellström, E., Nikulin, G. and Wyser, K.: The Rossby Centre Regional Climate model RCA3: model description and performance, Tellus, 63, 4-23, doi: 10.1111/j.1600-0870.2010.00478.x, 2010.

Seguro, J.V., and Lambert, T.W.: Modern estimation of the parameters of the Weibull wind speed distribution for wind energy analysis, J. Wind Eng. Ind. Aerod., 85, 75–84, 2000.

Skydd & Säkerhet, The cost of the forest fire is approaching one billion, available at: http://skyddosakerhet.se/nyheter/kostnader-skogsbranden-narmar-sig-en-miljard/ (last access: 3 September 2014), 2014 (in Swedish).

SOU 2007: Sweden facing climate change - threats and opportunities. Final report from the Swedish Commission on Climate and Vulnerability, Stockholm 2007.

Stocks, B.J., Lawson, B.D., Alexander, M.E., Van Wagner, C.E., McAlpine, R.S, Lynham, T.J. and Dubé, D.E.: The Canadian Forest Fire Danger Rating System: An Overview, Forest. Chron., 65, 450-457, 1989.

Themeßl, M.J., Gobiet, A., and Leuprecht, A.: Empirical-statistical downscaling and error correction of daily precipitation from regional climate models, Int. J. Climatol., 31, 1530–1544, 2011.

Turner, J.A.: The drought code component of the Canadian forest fire behavior system. Environment Canada, Publication No. 1316, Canadian Forestry Service, Headquarters, Ottawa, 14 pp., 1972.

Van Wagner, C.E.: Development and structure of the Canadian Forest Fire Weather Index system, Forestry Technical Report 35, Canadian Forest Service, Ottawa, Canada, 1987.

Viegas, D.X., Bovio, G., Ferreira, A., Nosenzo, A. and Sol, B.: Comparative study of various methods of fire danger evaluation in southern Europe, Int. J. Wildland Fire, 10, 235-246, 1999.

~~Viney, N.R.: A Review of Fine Fuel Moisture Modelling, Int. J. Wildland Fire 1, 215-234, 1991.~~

Wotton, B.M., Martell, D.L. and Logan, K.A.: Climate change and people-caused forest fire occurrence in Ontario, Climatic change, 60, 275-295, 2003.

Wilcke, R.A.I., Mendlik, T., Gobiet, A.: Multi-Variable Error-Correction of Regional Climate Models, Climatic Change, 120, 871-887, 2013.

Willén, U.: Preliminary use of CM-SAF cloud and radiation products for evaluation of regional climate simulations. SMHI Rep. Meteorol. Climatol., 131, Swedish meteorological and hydrological institute (SMHI), Sweden, 2008.

Yang, W., Andréasson, J., Graham, L.P., Olsson, J., Rosberg, J and Wetterhall, F.: Distribution based scaling to improve usability of regional climate model projections for hydrological climate change impacts studies, Hydrol. Res., 41..3-4, 2010.

Yao, A.Y.M.: A statistical model for the surface relative humidity, J. Appl. Meteorol., 13, 17-21, 1974.

**Table 1. Range of FWI for fire danger classes in Sweden.**

| Danger class (FWIX) | FWI range |
|---|---|
| 6 (5E) - Extremely high *) | 28 ≤ FWI |
| 5 - Very high | 22 ≤ FWI < 28 |
| 4 - High | 17 ≤ FWI < 22 |
| 3 - Normal | 7 ≤ FWI < 17 |
| 2 - Low | 1 ≤ FWI < 7 |
| 1 - Very low | FWI < 1 |

*) ***in operational use. danger class 6***

**Table 2. Statistical characteristics of *P, T, H* and *W* during the calibration period (1966-1985) over all stations. Comparison between observation, raw RCA3-ERA40 and raw RCA3-E5r3A1B. The bold number in brackets presents the biases between modelled value and observed value in % except Avg. of *T*.**

| | | ***P*** | | | | ***T*** | | | ***H*** | | | ***W*** | | | |
|---|---|---|---|---|---|---|---|---|---|---|---|---|---|---|---|
| | | Acc. **[mm]** | $SD^1$ **[-]** | $SD^2$ **[-]** | Freq-P **[%]** | Avg **[º C]** | $SD^1$ **[-]** | $SD^2$ **[-]** | Avg **(%)** | $SD^1$ **[-]** | $SD^2$ **[-]** | Avg **[m/s]** | $SD^1$ **[-]** | $SD^2$ **[-]** | Freq-Ws **[%]** |
| MAM | Observation | 82.3 | 3.2 | 20.0 | 42.8 | 6.6 | 6.5 | 1.9 | 63.6 | 18.6 | 3.1 | 4.0 | 2.4 | 0.8 | 92.1 |
| | RCA3-ERA40 | 175.4 **(+113.1)** | 3.1 **(-3.1)** | 21.4 **(+7.0)** | 77.4 **(+80.8)** | 5.0 **(-1.6)** | 5.4 **(-16.9)** | 2.5 **(+31.6)** | 66.4 **(+4.4)** | 19.0 **(+2.2)** | 7.7 **(+148.4)** | 3.2 **(-20.0)** | 1.4 **(-41.7)** | 0.2 **(-75.0)** | 100.0 **(+8.6)** |
| | RCA3-E5r3A1B | 183.8 **(+123.3)** | 3.2 **(-)** | 23.0 **(+15.0)** | 77.4 **(+80.8)** | 5.0 **(-1.6)** | 5.5 **(-15.4)** | 2.4 **(+26.3)** | 67.9 **(+6.8)** | 18.9 **(+1.6)** | 7.3 **(+135.5)** | 3.1 **(-22.5)** | 1.4 **(-41.7)** | 0.2 **(-75.0)** | 100.0 **(+8.6)** |
| JJA | Observation | 143.9 | 5.0 | 28.0 | 43.7 | 18.3 | 4.3 | 1.4 | 57.6 | 16.5 | 3.3 | 3.8 | 2.2 | 0.8 | 90.6 |
| | RCA3-ERA40 | 265.5 **(+84.5)** | 4.8 **(-4.0)** | 32.1 **(+14.6)** | 86.5 **(+97.9)** | 16.0 **(-2.3)** | 2.8 **(-34.9)** | 1.8 **(+28.6)** | 68.4 **(+18.8)** | 17.5 **(+6.1)** | 4.5 **(+36.4)** | 2.6 **(-31.6)** | 1.2 **(-45.5)** | 0.2 **(-75.0)** | 100.0 **(+10.4)** |
| | RCA3-E5r3A1B | 313.9 **(+118.1)** | 4.8 **(-4.0)** | 41.5 **(+48.2)** | 89.9 **(+105.7)** | 15.0 **(-3.3)** | 2.5 **(-41.9)** | 1.5 **(+7.1)** | 71.5 **(+24.1)** | 17.5 **(+6.1)** | 3.6 **(+9.1)** | 2.7 **(-28.9)** | 1.3 **(-40.9)** | 0.3 **(-62.5)** | 100.0 **(+10.4)** |
| SON | Observation | 166.6 | 4.4 | 38.6 | 54.3 | 7.2 | 6.2 | 2.6 | 75.4 | 16.3 | 2.1 | 3.7 | 2.6 | 1.1 | 88.3 |
| | RCA3-ERA40 | 267.1 **(+60.3)** | 3.9 **(-11.4)** | 27.8 **(-28.0)** | 90.5 **(+66.7)** | 6.3 **(-0.9)** | 5.3 **(-14.5)** | 2.4 **(-7.7)** | 80.6 **(+6.7)** | 15.9 **(-2.5)** | 1.8 **(-14.3)** | 3.2 **(-13.5)** | 1.5 **(-42.3)** | 0.4 **(-63.6)** | 100.0 **(+13.3)** |
| | RCA3-E5r3A1B | 287.6 **(+72.6)** | 4.1 **(-6.8)** | 27.1 **(-29.8)** | 92.6 **(+70.5)** | 6.7 **(-0.5)** | 4.7 **(-24.2)** | 2.2 **(-15.4)** | 82.3 **(+9.2)** | 15.1 **(-7.4)** | 1.8 **(-14.3)** | 3.2 **(-13.5)** | 1.4 **(-46.2)** | 0.4 **(-63.6)** | 100.0 **(+13.3)** |

**Table 3. PDF skill scores (SS) of raw data from RCA3-ERA40 and RCA3-E5r3-A1B (1966-1985), averaged over all stations.**

| | | Precipitation | | | Temperature | | | Relative humidity | | | Wind speed | | |
|---|---|---|---|---|---|---|---|---|---|---|---|---|---|
| | | Mean | Min. | Max | Mean | Min. | Max | Mean | Min | Max | Mean | Min | Max |
| MAM | RCA3-ERA40 | 0.64 | 0.59 | 0.69 | 0.80 | 0.74 | 0.86 | 0.83 | 0.76 | 0.87 | 0.75 | 0.65 | 0.84 |
| | RCA3-E5r3A1B | 0.65 | 0.60 | 0.70 | 0.80 | 0.75 | 0.85 | 0.81 | 0.76 | 0.86 | 0.69 | 0.57 | 0.76 |
| JJA | RCA3-ERA40 | 0.56 | 0.48 | 0.60 | 0.71 | 0.67 | 0.76 | 0.72 | 0.63 | 0.78 | 0.70 | 0.55 | 0.83 |
| | RCA3-E5r3A1B | 0.54 | 0.45 | 0.60 | 0.59 | 0.54 | 0.63 | 0.67 | 0.60 | 0.72 | 0.66 | 0.52 | 0.76 |
| SON | RCA3-ERA40 | 0.62 | 0.58 | 0.58 | 0.85 | 0.89 | 0.81 | 0.78 | 0.74 | 0.89 | 0.76 | 0.62 | 0.86 |
| | RCA3-E5r3A1B | 0.61 | 0.68 | 0.65 | 0.82 | 0.79 | 0.79 | 0.74 | 0.69 | 0.84 | 0.68 | 0.58 | 0.83 |

**Table 4. PDF skill scores (SS) of data from raw and corrected RCA3-E5r3A1B (1986-2005), averaged over all stations.**

| | | Precipitation | | | Temperature | | | Relative humidity | | | Wind speed | | |
|---|---|---|---|---|---|---|---|---|---|---|---|---|---|
| | | Mean | Min. | Max | Mean | Min. | Max | Mean | Min | Max | Mean | Min | Max |
| MAM | Raw | 0.62 | 0.58 | 0.65 | 0.78 | 0.74 | 0.85 | 0.75 | 0.66 | 0.81 | 0.73 | 0.60 | 0.88 |
| | Corrected | 0.93 | 0.86 | 0.96 | 0.89 | 0.83 | 0.91 | 0.84 | 0.75 | 0.88 | 0.82 | 0.73 | 0.93 |
| JJA | Raw | 0.57 | 0.53 | 0.60 | 0.58 | 0.53 | 0.61 | 0.66 | 0.57 | 0.73 | 0.64 | 0.51 | 0.77 |
| | Corrected | 0.93 | 0.91 | 0.95 | 0.91 | 0.89 | 0.93 | 0.81 | 0.75 | 0.86 | 0.83 | 0.73 | 0.94 |
| SON | Raw | 0.60 | 0.57 | 0.62 | 0.83 | 0.80 | 0.86 | 0.72 | 0.66 | 0.78 | 0.77 | 0.63 | 0.92 |
| | Corrected | 0.93 | 0.91 | 0.95 | 0.90 | 0.86 | 0.92 | 0.83 | 0.77 | 0.89 | 0.84 | 0.77 | 0.92 |


**Figure 1. Map showing the locations of the observation stations**

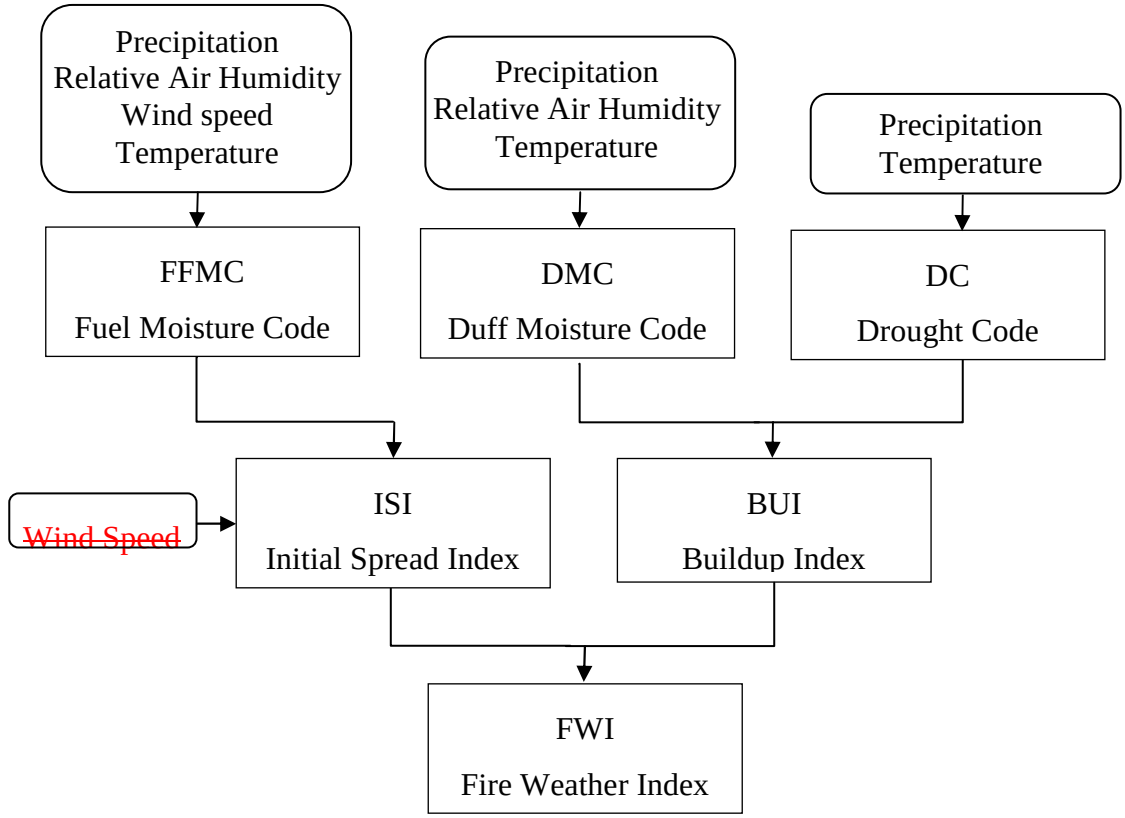


Figure 2. The structure of the Fire Weather Index (FWI) system

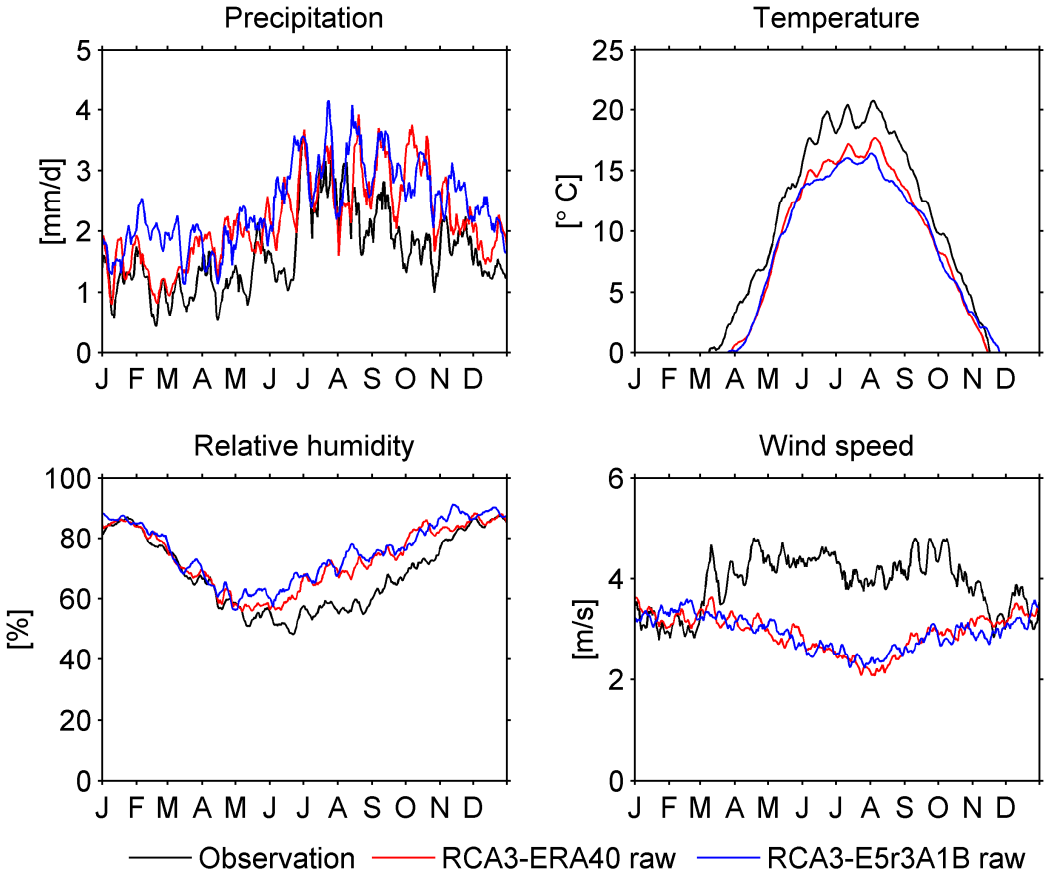


**Figure 2~~Figure 3~~. Seasonal variation of the FWI inputs (*P*, *T*, *H* and *W*) presented as 7-day moving average value at Edsbyn station. Comparison of observational data and raw output of the climate models from RCA3-ERA40 and RCA3-E5r3-A1B simulations (calibration period 1966-1985).**

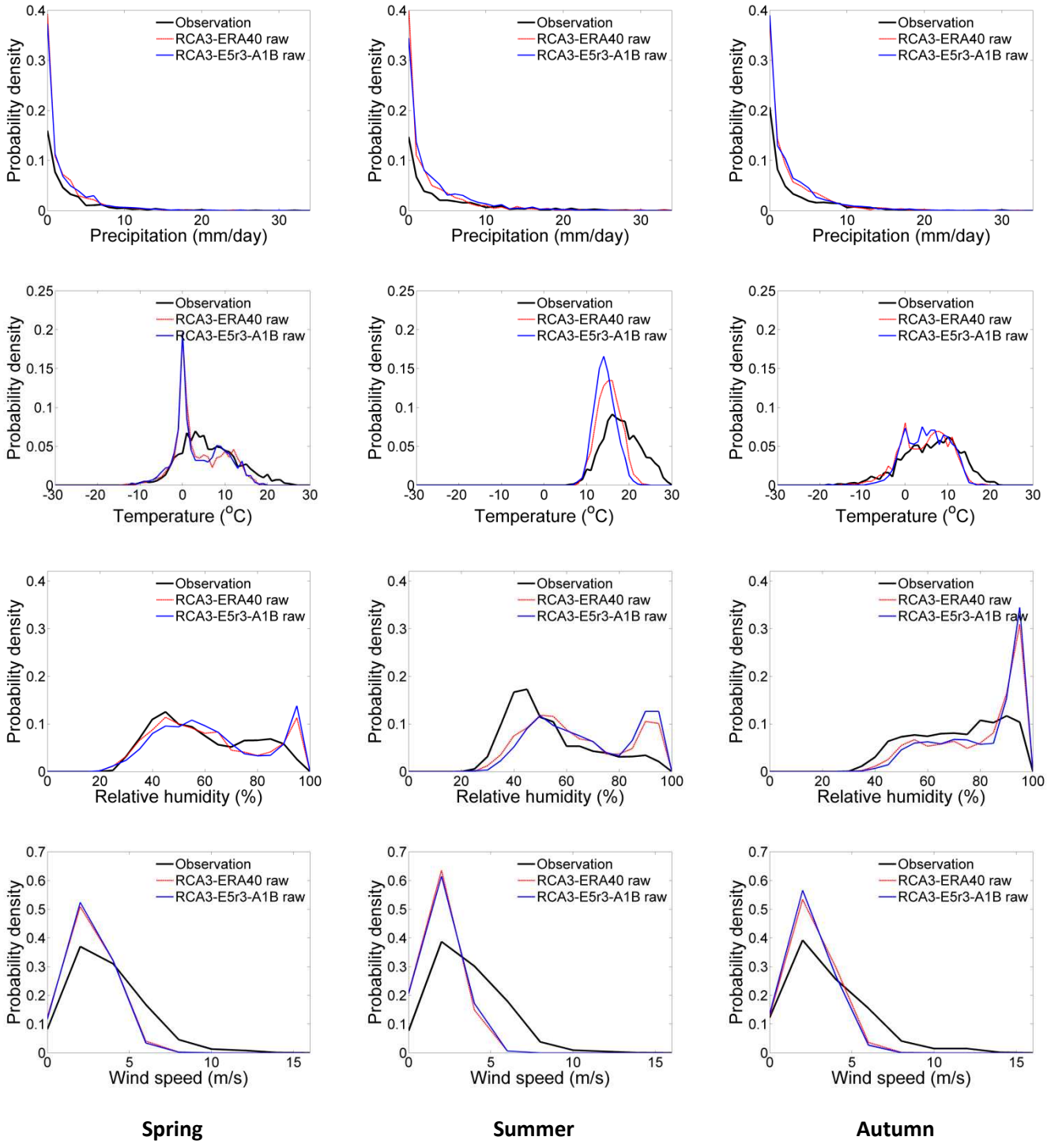


**Figure 3~~Figure 4~~. Probability density functions of precipitation, temperature, relative humidity and wind speed at Edsbyn station. Comparison of observational data and raw output of the climate models RCA3-ERA40 and RCA3-E5r3-A1B (1966-1985).**

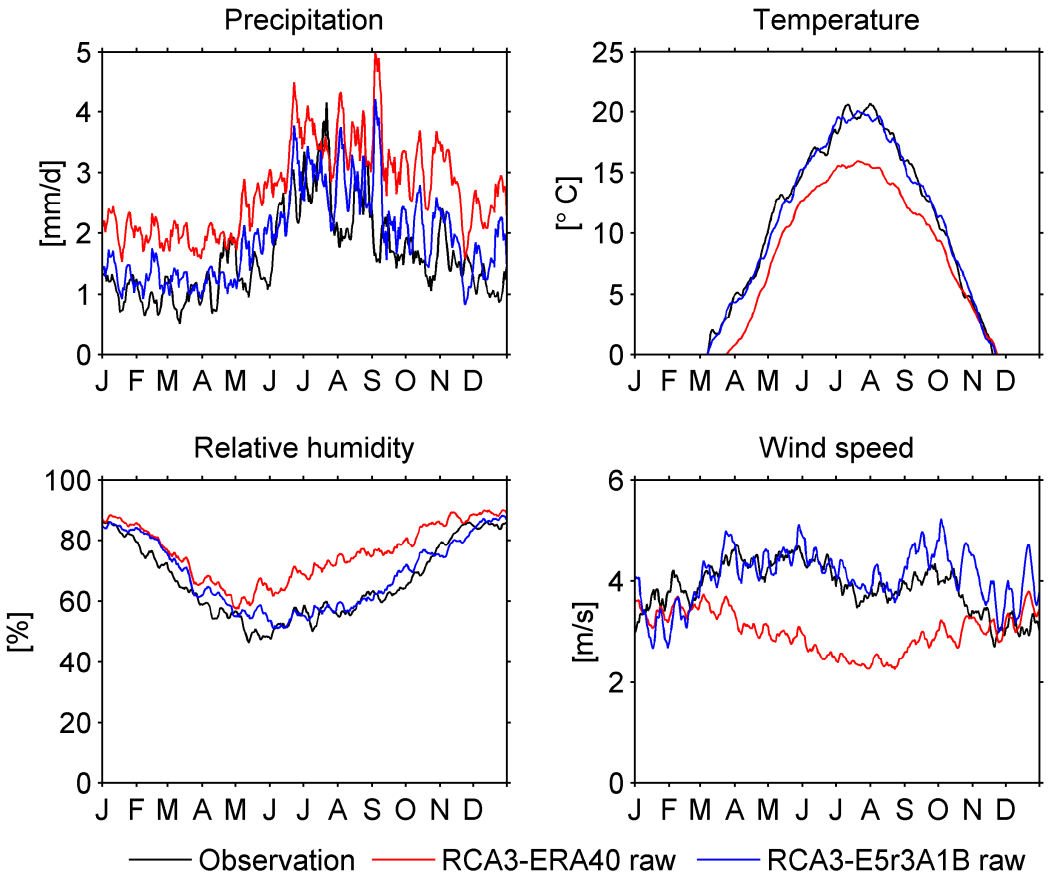


**Figure 4~~Figure 5~~. Seasonal variation of the FWI inputs (*P*, *T*, *H* and *W*) presented as 7-day moving average value at Edsbyn station. Comparison of observational data, raw output of the climate models from RCA3-E5r3-A1B simulation, and its corresponding corrected output (validation period 1986-2005).**

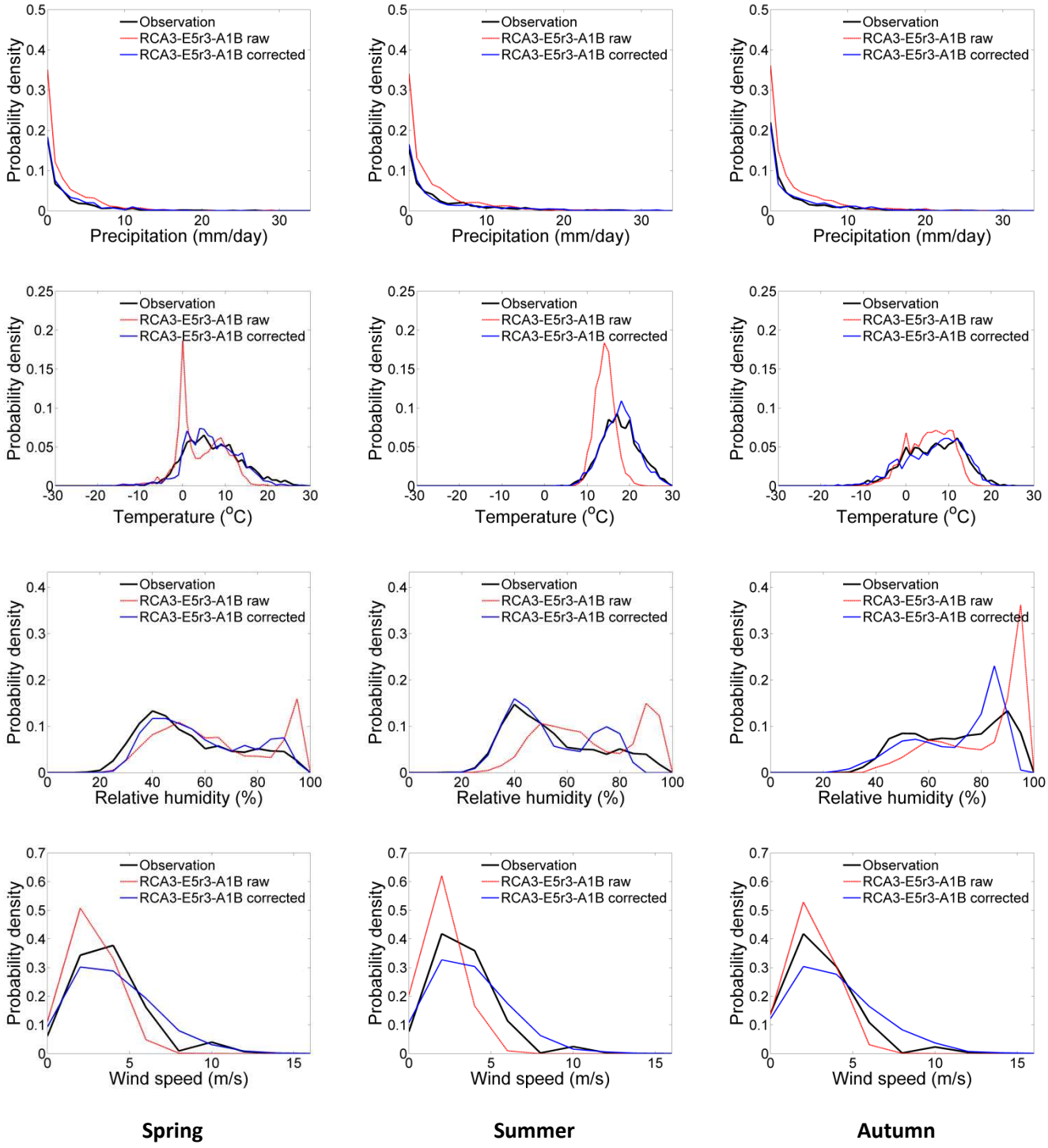


**Figure 5~~Figure 6~~. Comparison of observational data, the raw output of the climate model, RCA3-E5r3A1B, and its corresponding adjusted output at Edsbyn station for validation period 1986-2005.**

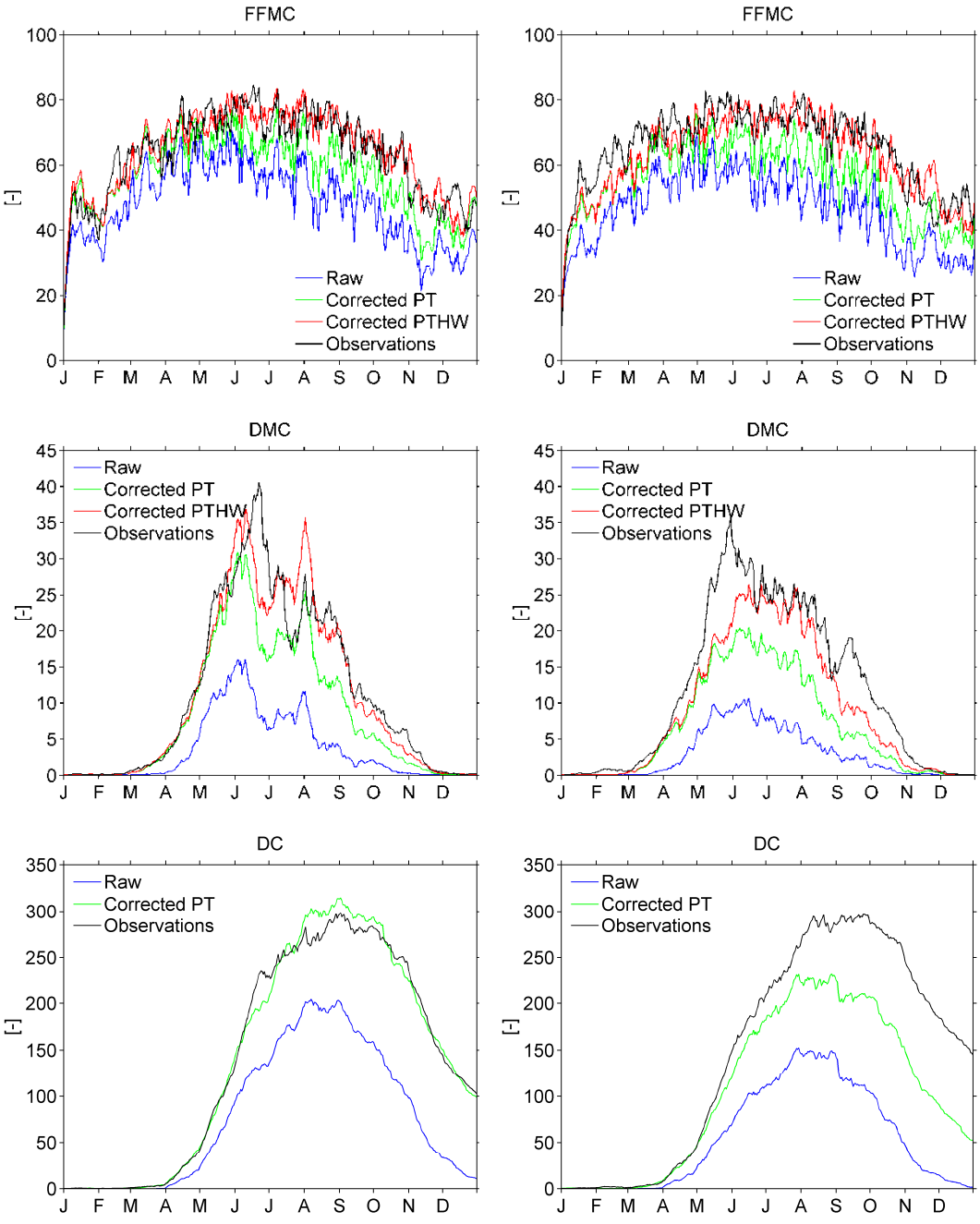


**Figure 6~~Figure 7~~. Seasonal variation of FFMC, DMC and DC index at Edsbyn station. Comparison of values based on observations (black line), raw output from climate model (blue line), RCA3-E5r3A1B, corrected *P* and *T* uncorrected *H*-raw and *W*-raw (green line) and corrected *P*, *T*, *H* and *W* (red line) for period a) 1966-1985 and b) 1986-2005. Note that the DC is influenced by *P* and *T* (see blue, green and black lines).**

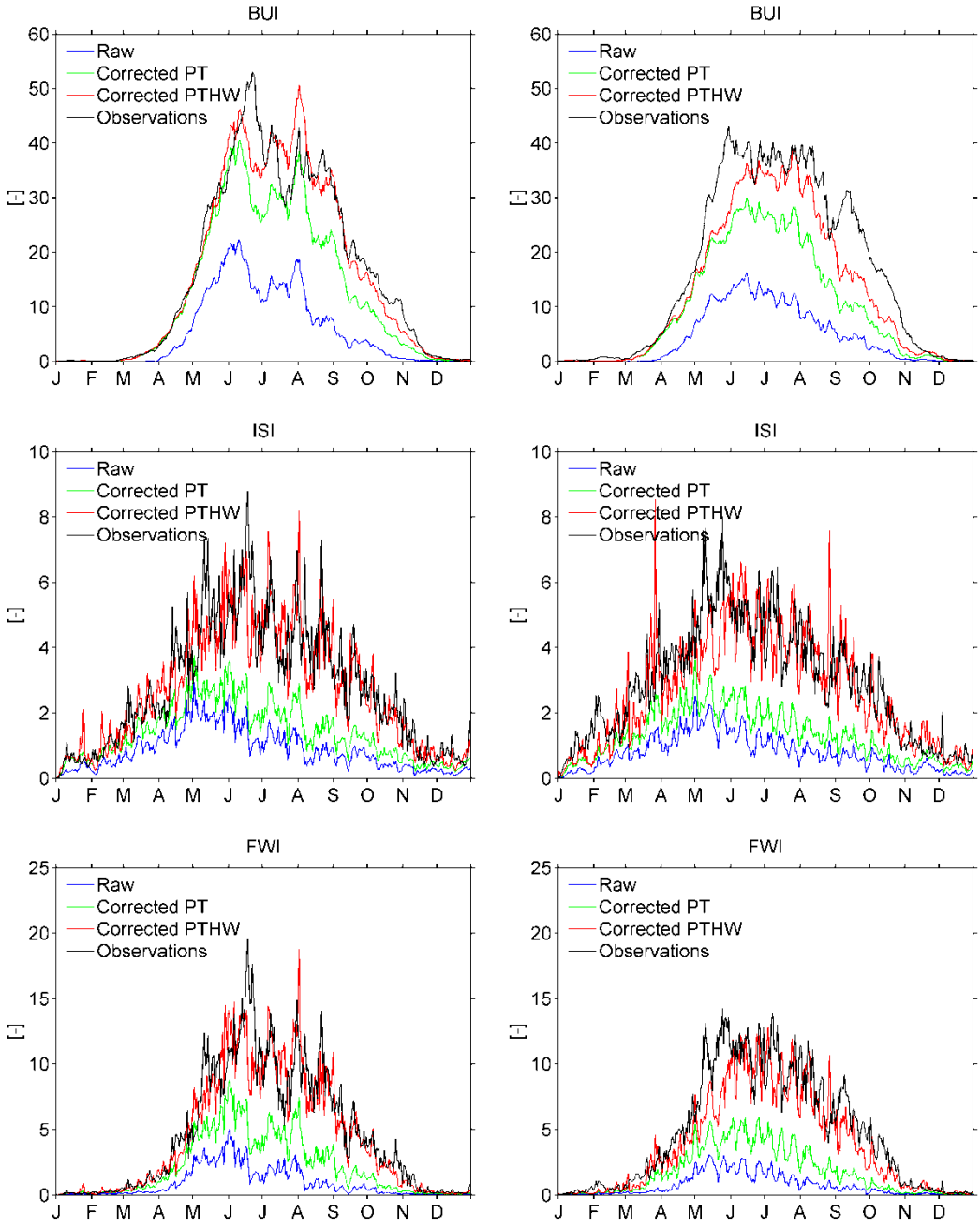


~~1~~a) 1966-1985 ~~2~~b) 1986-2005

**Figure 7~~Figure 8~~. Seasonal variation of BUI, ISI and FWI index at Edsbyn station. Comparison of values based on observations (black line), raw output from climate model (blue line), RCA3-E5r3A1B, corrected *P* and *T* uncorrected (raw) *H* and *W* (green line) and corrected *P*, *T*, *H* and *W* (red line) for period a) 1966-1985 and b) 1986-2005.**

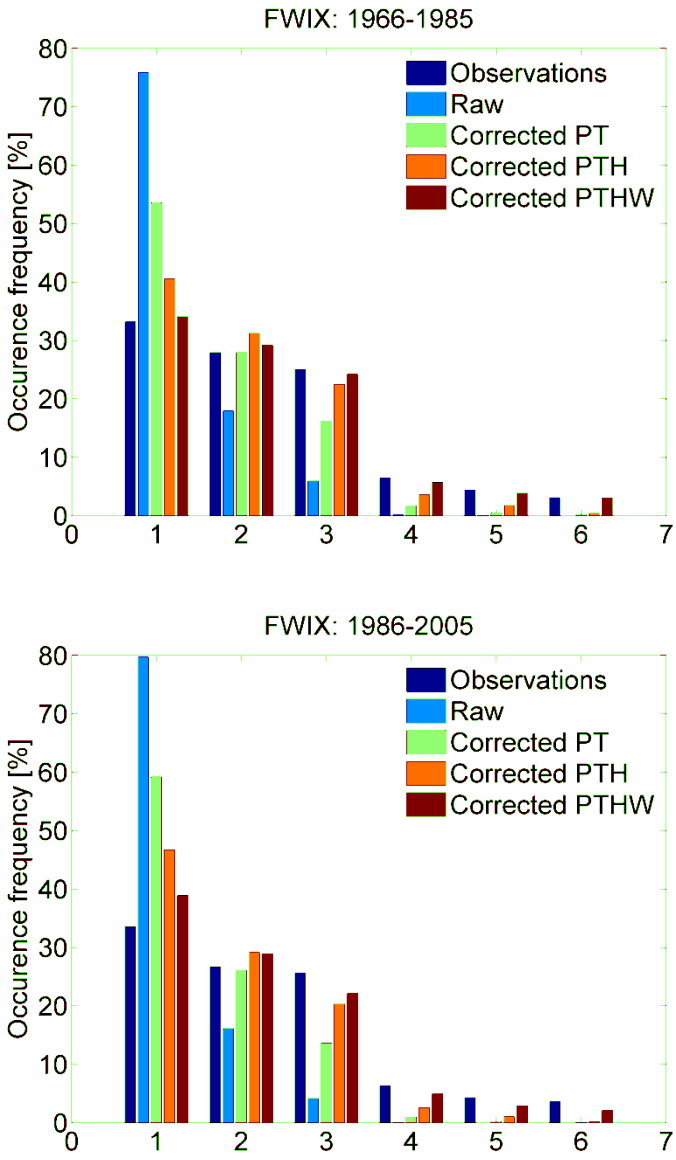


**Figure 8~~Figure 9~~. The occurrence frequency of fire danger classes (i.e., FWIX) at Edsbyn station calculated from observation, raw climate model output, RCA3-E5r3A1B, and after correcting meteorological variables.**

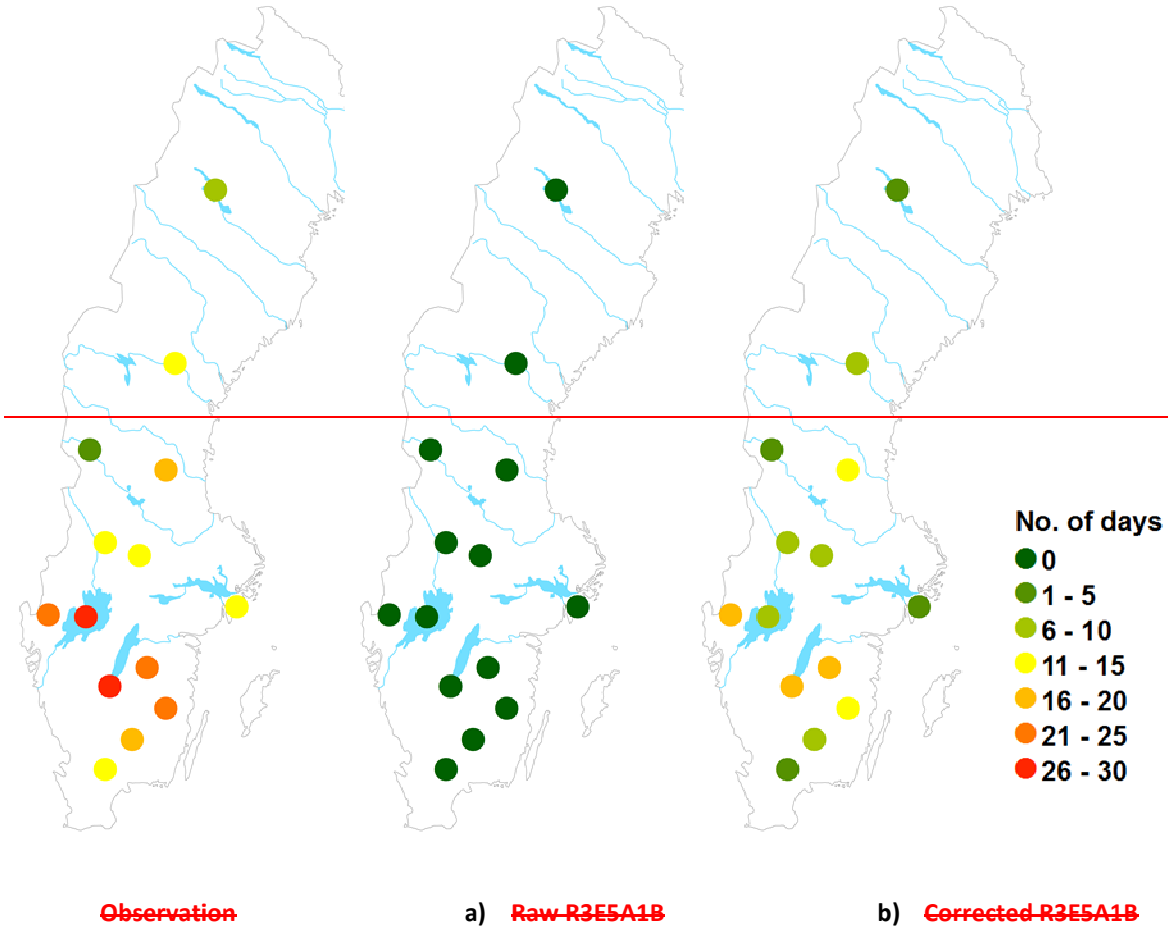


Figure 10. Annual mean of number of days with high fire risk (FWIX >= 5) during the calibration period (1966-1985)

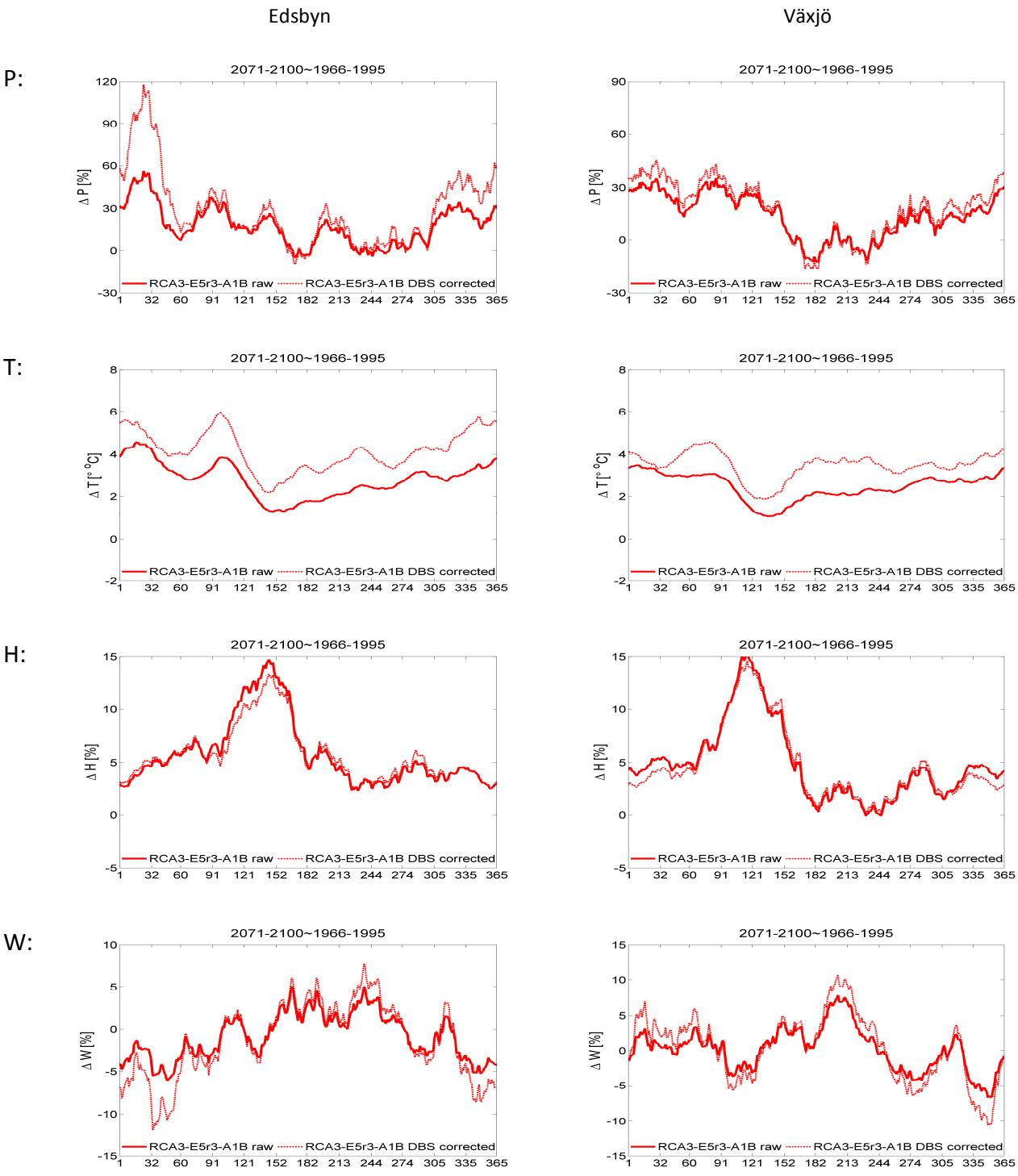


**Figure 9~~Figure 11~~. Climate change signals in *P*, *T*, *H* and *W* at Edsbyn and Växjö station, reflected in RCA3-E5r3-A1B before and after correction during ~~three periods, 2011-2040, 2041-2070 and~~ 2071-2100 ~~(from top to bottom)~~.**

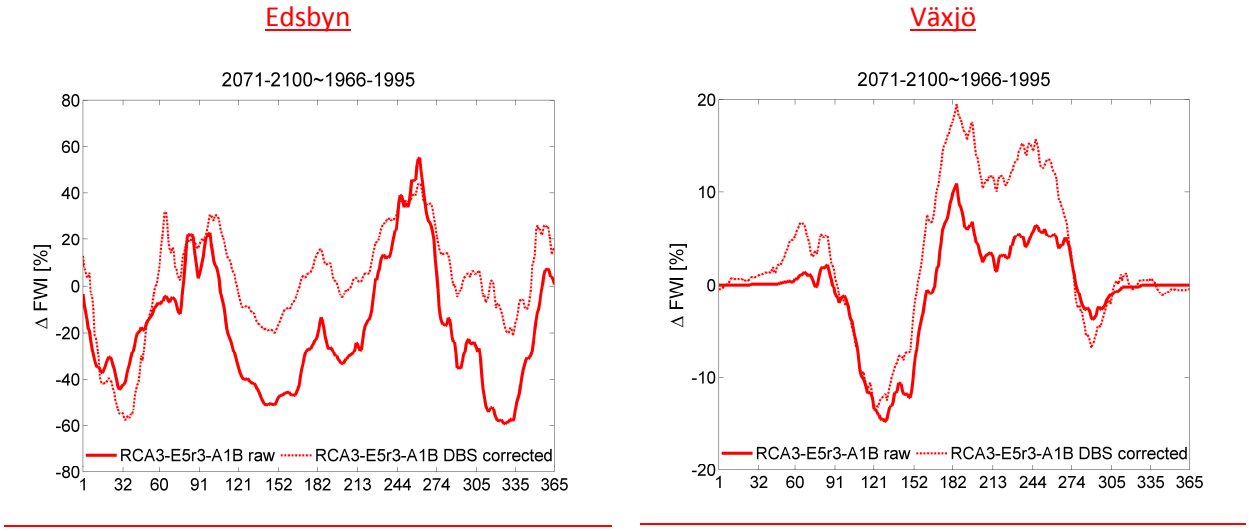


**Figure 10~~Figure 13~~. Climate change (CC) signals in the FWI reflected in RCA3-E5r3-A1B during the period of ~~2011-2040, 2041-2070 and~~ 2071-2100 at Edsbyn and Växjö station ~~(from top to bottom panel)~~.**

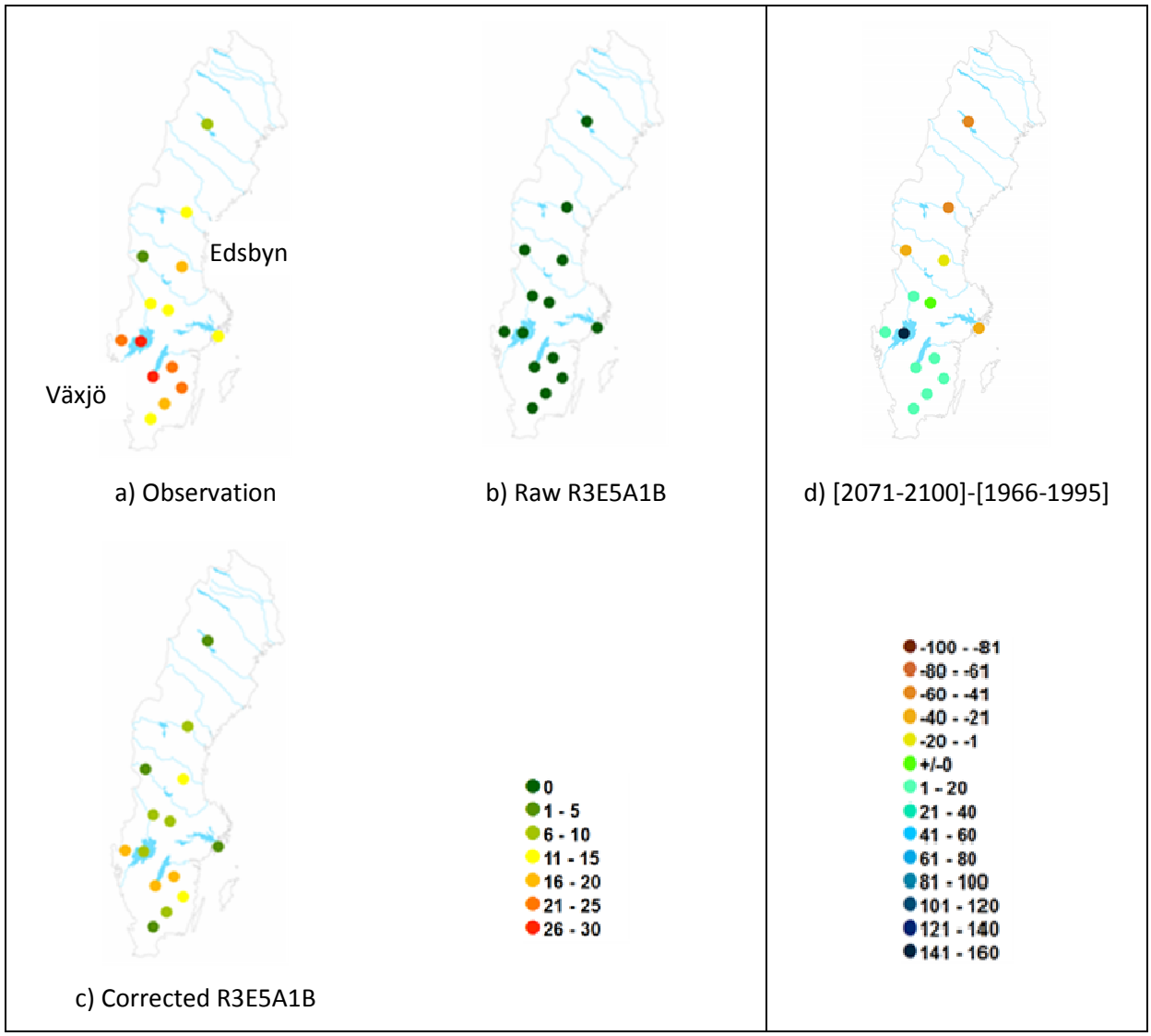


**Figure 11. Number of days during the calibration period (1966-1995) presented by a) observation, b) Raw R3E5A1B and c) Corrected raw R3E5A1B; and changes of number of days in percentage during the period of d) 2071-2100.**